

FEATURES

- Extremely high 97% efficiency**
- Ultralow quiescent current: 20 μ A**
- 1.2 MHz switching frequency**
- 0.1 μ A shutdown supply current**
- Maximum load current**
 - ADP2105: 1 A**
 - ADP2106: 1.5 A**
 - ADP2107: 2 A**
- Input voltage: 2.7 V to 5.5 V**
- Output voltage: 0.8 V to V_{IN}**
- Maximum duty cycle: 100%**
- Smoothly transitions into low dropout (LDO) mode**
- Internal synchronous rectifier**
- Small 16-lead 4 mm \times 4 mm LFCSP_VQ package**
- Optimized for small ceramic output capacitors**
- Enable/shutdown logic input**
- Undervoltage lockout**
- Soft start**
- Supported by ADIsimPower™ design tool**

APPLICATIONS

- Mobile handsets**
- PDA's and palmtop computers**
- Telecommunication/networking equipment**
- Set top boxes**
- Audio/video consumer electronics**

GENERAL DESCRIPTION

The ADP2105/ADP2106/ADP2107 are low quiescent current, synchronous, step-down dc-to-dc converters in a compact 4 mm \times 4 mm LFCSP_VQ package. At medium to high load currents, these devices use a current mode, constant frequency pulse-width modulation (PWM) control scheme for excellent stability and transient response. To ensure the longest battery life in portable applications, the ADP2105/ADP2106/ADP2107 use a pulse frequency modulation (PFM) control scheme under light load conditions that reduces switching frequency to save power.

The ADP2105/ADP2106/ADP2107 run from input voltages of 2.7 V to 5.5 V, allowing single Li+/Li- polymer cell, multiple alkaline/NiMH cells, PCMCIA, and other standard power sources. The output voltage of ADP2105/ADP2106/ADP2107 is adjustable from 0.8 V to the input voltage (indicated by ADJ), whereas the ADP2105/ADP2106/ADP2107 are available in preset output voltage options of 3.3 V, 1.8 V, 1.5 V, and 1.2 V (indicated by x.x V). Each of these variations is available in three maximum current levels: 1 A (ADP2105), 1.5 A (ADP2106), and 2 A (ADP2107). The power switch and synchronous rectifier are integrated for minimal external part count and high efficiency. During logic controlled shutdown, the input is disconnected from the output, and it draws less than 0.1 μ A from the input source. Other key features include undervoltage lockout to prevent deep battery discharge and programmable soft start to limit inrush current at startup.

TYPICAL OPERATING CIRCUIT

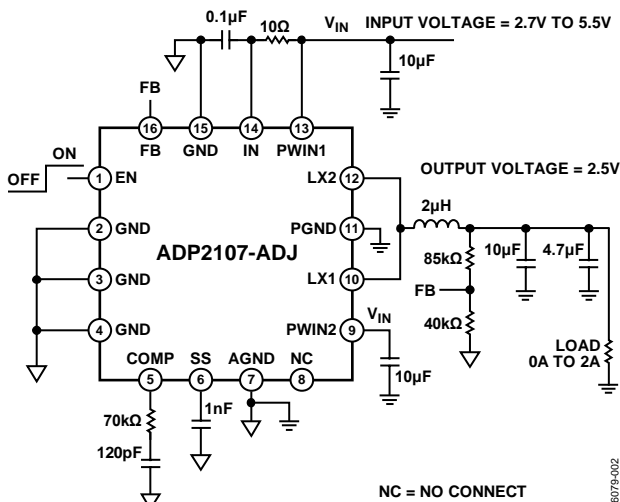


Figure 1. Circuit Configuration of ADP2107 with $V_{OUT} = 2.5$ V

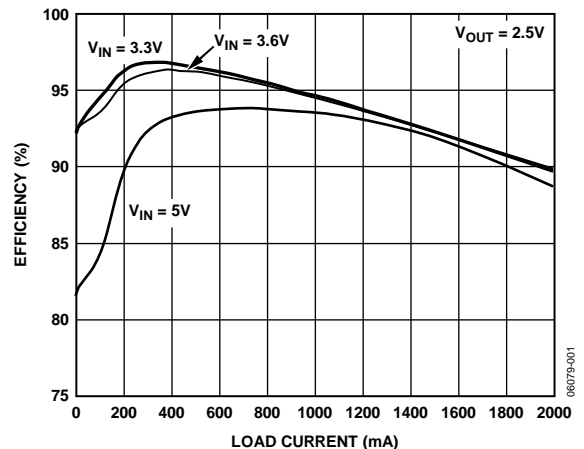


Figure 2. Efficiency vs. Load Current for the ADP2107 with $V_{OUT} = 2.5$ V

Rev. D

Information furnished by Analog Devices is believed to be accurate and reliable. However, no responsibility is assumed by Analog Devices for its use, nor for any infringements of patents or other rights of third parties that may result from its use. Specifications subject to change without notice. No license is granted by implication or otherwise under any patent or patent rights of Analog Devices. Trademarks and registered trademarks are the property of their respective owners.

TABLE OF CONTENTS

Features	1	External Component Selection	16
Applications	1	Setting the Output Voltage	16
General Description	1	Inductor Selection	17
Typical Operating Circuit	1	Output Capacitor Selection	18
Revision History	2	Input Capacitor Selection	19
Functional Block Diagram	3	Input Filter	19
Specifications	4	Soft Start Period	19
Absolute Maximum Ratings	6	Loop Compensation	19
Thermal Resistance	6	Bode Plots	20
Boundary Condition	6	Load Transient Response	21
ESD Caution	6	Efficiency Considerations	22
Pin Configuration and Function Descriptions	7	Thermal Considerations	22
Typical Performance Characteristics	8	Design Example	24
Theory of Operation	14	External Component Recommendations	25
Control Scheme	14	Circuit Board Layout Recommendations	27
PWM Mode Operation	14	Evaluation Board	28
PFM Mode Operation	14	Evaluation Board Schematic for ADP2107 (1.8 V)	28
Pulse-Skipping Threshold	14	Recommended PCB Board Layout (Evaluation Board Layout)	28
100% Duty Cycle Operation (LDO Mode)	14	Application Circuits	30
Slope Compensation	15	Outline Dimensions	33
Design Features	15	Ordering Guide	33
Applications Information	16		

REVISION HISTORY

8/12—Rev. C to Rev. D

Change to Features Section	1
Added Exposed Pad Notation to Pin Configuration and Function Description Section	7
Added ADIsimPower Design Tool Section	16
Updated Outline Dimensions	33

9/08—Rev. B to Rev. C

Changes to Table Summary Statement	4
Changes to LX Minimum On-Time Parameter, Table 1	5

7/08—Rev. A to Rev. B

Changes to General Description Section	1
Changes to Figure 3	3
Changes to Table 1	4
Changes to Table 2	6
Changes to Figure 4	7
Changes to Table 4	7
Changes to Figure 26	11
Changes to Figure 31 Through Figure 34	12
Changes to Figure 35	13
Changes to PMW Mode Operation Section and Pulse Skipping Threshold Section	14

Changes to Slope Compensation Section	15
Changes to Setting the Output Voltage Section	16
Changes to Figure 37	16
Changes to Inductor Selection Section	17
Changes to Input Capacitor Selection Section	18
Changes to Figure 47 through Figure 52	21
Changes to Transition Losses Section and Thermal Considerations Section	22
Changes to Table 11	25
Changes to Circuit Board Layout Recommendations Section	27
Changes to Table 12	26
Changes to Figure 53	28
Changes to Figure 56 Through Figure 57	30
Changes to Figure 58 Through Figure 59	31
Changes to Outline Dimensions	33

3/07—Rev. 0 to Rev. A

Updated Format	Universal
Changes to Output Characteristics and LX (Switch Node) Characteristics Sections	3
Changes to Typical Performance Characteristics Section	7
Changes to Load Transient Response Section	21

7/06—Revision 0: Initial Version

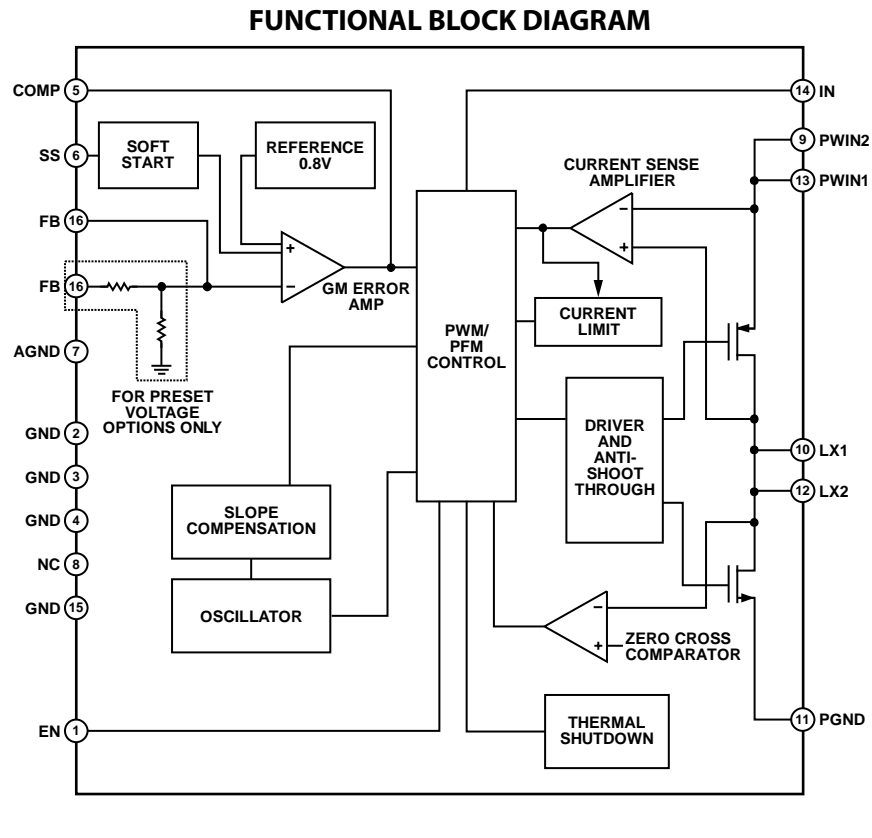


Figure 3.

SPECIFICATIONS

$V_{IN} = 3.6 \text{ V}$ @ $T_A = 25^\circ\text{C}$, unless otherwise noted.¹

Table 1.

Parameter	Min	Typ	Max	Unit	Conditions
INPUT CHARACTERISTICS					
Input Voltage Range	2.7		5.5	V	$-40^\circ\text{C} \leq T_J \leq +125^\circ\text{C}$
Undervoltage Lockout Threshold		2.4		V	V_{IN} rising
	2.2		2.6	V	V_{IN} rising, $-40^\circ\text{C} \leq T_J \leq +125^\circ\text{C}$
Undervoltage Lockout Hysteresis ²		2.2		V	V_{IN} falling
	2.0		2.5	V	V_{IN} falling, $-40^\circ\text{C} \leq T_J \leq +125^\circ\text{C}$
OUTPUT CHARACTERISTICS					
Output Regulation Voltage	3.267	3.3	3.333	V	3.3 V, load = 10 mA
		3.3		V	3.3 V, $V_{IN} = 3.6 \text{ V}$ to 5.5 V, no load to full load
	3.201		3.399	V	3.3 V, $V_{IN} = 3.6 \text{ V}$ to 5.5 V, no load to full load, $-40^\circ\text{C} \leq T_J \leq +125^\circ\text{C}$
	1.782	1.8	1.818	V	1.8 V, load = 10 mA
		1.8		V	1.8 V, $V_{IN} = 2.7 \text{ V}$ to 5.5 V, no load to full load
	1.746		1.854	V	1.8 V, $V_{IN} = 2.7 \text{ V}$ to 5.5 V, no load to full load, $-40^\circ\text{C} \leq T_J \leq +125^\circ\text{C}$
	1.485	1.5	1.515	V	1.5, load = 10 mA
		1.5		V	ADP210x-1.5 V, $V_{IN} = 2.7 \text{ V}$ to 5.5 V, no load to full load
	1.455		1.545	V	ADP210x-1.5 V, $V_{IN} = 2.7 \text{ V}$ to 5.5 V, no load to full load, $-40^\circ\text{C} \leq T_J \leq +125^\circ\text{C}$
	1.188	1.2	1.212	V	1.2 V, load = 10 mA
Load Regulation		0.4		%/A	ADP2105
		0.5		%/A	ADP2106
Line Regulation ³		0.6		%/A	ADP2107
		0.1	0.33	%/V	ADP2105, measured in servo loop
Output Voltage Range		0.1	0.3	%/V	ADP2106 and ADP2107, measured in servo loop
	0.8		V_{IN}	V	ADJ
FEEDBACK CHARACTERISTICS					
FB Regulation Voltage		0.8		V	ADJ
	0.784		0.816	V	ADJ, $-40^\circ\text{C} \leq T_J \leq +125^\circ\text{C}$
FB Bias Current	-0.1		+0.1	μA	ADJ, $-40^\circ\text{C} \leq T_J \leq +125^\circ\text{C}$
		3		μA	1.2 V output voltage
			6	μA	1.2 V output voltage, $-40^\circ\text{C} \leq T_J \leq +125^\circ\text{C}$
		4		μA	1.5 V output voltage
			8	μA	1.5 V output voltage, $-40^\circ\text{C} \leq T_J \leq +125^\circ\text{C}$
		5		μA	1.8 V output voltage
			10	μA	1.8 V output voltage, $-40^\circ\text{C} \leq T_J \leq +125^\circ\text{C}$
	10		μA	3.3 V output voltage	
		20	μA	3.3 V output voltage, $-40^\circ\text{C} \leq T_J \leq +125^\circ\text{C}$	

Parameter	Min	Typ	Max	Unit	Conditions	
INPUT CURRENT CHARACTERISTICS						
IN Operating Current		20		μA	ADP210x(ADJ), $V_{\text{FB}} = 0.9\text{ V}$	
			30	μA	ADP210x(ADJ), $V_{\text{FB}} = 0.9\text{ V}$, $-40^\circ\text{C} \leq T_j \leq +125^\circ\text{C}$	
		20		μA	ADP210x(x.x V) output voltage 10% above regulation voltage	
			30	μA	ADP210x(x.x V) output voltage 10% above regulation voltage, $-40^\circ\text{C} \leq T_j \leq +125^\circ\text{C}$	
IN Shutdown Current ⁴		0.1	1	μA	$V_{\text{EN}} = 0\text{ V}$	
LX (SWITCH) NODE CHARACTERISTICS						
LX On Resistance ⁴		190		$\text{m}\Omega$	P-channel switch, ADP2105	
			270	$\text{m}\Omega$	P-channel switch, ADP2105, $-40^\circ\text{C} \leq T_j \leq +125^\circ\text{C}$	
		100		$\text{m}\Omega$	P-channel switch, ADP2106 and ADP2107	
			165	$\text{m}\Omega$	P-channel switch, ADP2106 and ADP2107, $-40^\circ\text{C} \leq T_j \leq +125^\circ\text{C}$	
		160		$\text{m}\Omega$	N-channel synchronous rectifier, ADP2105	
			230	$\text{m}\Omega$	N-channel synchronous rectifier, ADP2105, $-40^\circ\text{C} \leq T_j \leq +125^\circ\text{C}$	
		90		$\text{m}\Omega$	N-channel synchronous rectifier, ADP2106 and ADP2107	
			140	$\text{m}\Omega$	N-channel synchronous rectifier, ADP2106 and ADP2107, $-40^\circ\text{C} \leq T_j \leq +125^\circ\text{C}$	
	LX Leakage Current ^{4,5}		0.1	1	μA	$V_{\text{IN}} = 5.5\text{ V}$, $V_{\text{LX}} = 0\text{ V}$, 5.5 V
	LX Peak Current Limit ⁵		2.9		A	P-channel switch, ADP2107
2.6			3.3	A	P-channel switch, ADP2107, $-40^\circ\text{C} \leq T_j \leq +125^\circ\text{C}$	
		2.25		A	P-channel switch, ADP2106	
2.0			2.6	A	P-channel switch, ADP2106, $-40^\circ\text{C} \leq T_j \leq +125^\circ\text{C}$	
		1.5		A	P-channel switch, ADP2105	
LX Minimum On-Time			1.8	A	P-channel switch, ADP2105, $-40^\circ\text{C} \leq T_j \leq +125^\circ\text{C}$	
			110	ns	In PWM mode of operation, $-40^\circ\text{C} \leq T_j \leq +125^\circ\text{C}$	
ENABLE CHARACTERISTICS						
EN Input High Voltage	2			V	$V_{\text{IN}} = 2.7\text{ V to }5.5\text{ V}$, $-40^\circ\text{C} \leq T_j \leq +125^\circ\text{C}$	
EN Input Low Voltage			0.4	V	$V_{\text{IN}} = 2.7\text{ V to }5.5\text{ V}$, $-40^\circ\text{C} \leq T_j \leq +125^\circ\text{C}$	
EN Input Leakage Current		-0.1		μA	$V_{\text{IN}} = 5.5\text{ V}$, $V_{\text{EN}} = 0\text{ V}$, 5.5 V	
	-1		+1	μA	$V_{\text{IN}} = 5.5\text{ V}$, $V_{\text{EN}} = 0\text{ V}$, 5.5 V , $-40^\circ\text{C} \leq T_j \leq +125^\circ\text{C}$	
OSCILLATOR FREQUENCY						
		1.2		MHz	$V_{\text{IN}} = 2.7\text{ V to }5.5\text{ V}$	
	1		1.4	MHz	$V_{\text{IN}} = 2.7\text{ V to }5.5\text{ V}$, $-40^\circ\text{C} \leq T_j \leq +125^\circ\text{C}$	
SOFT START PERIOD	750	1000	1200	μs	$C_{\text{SS}} = 1\text{ nF}$	
THERMAL CHARACTERISTICS						
Thermal Shutdown Threshold		140		$^\circ\text{C}$		
Thermal Shutdown Hysteresis		40		$^\circ\text{C}$		
COMPENSATOR TRANSCONDUCTANCE (g_m)		50		$\mu\text{A/V}$		
CURRENT SENSE AMPLIFIER GAIN (G_{CS}) ²		1.875		A/V	ADP2105	
		2.8125		A/V	ADP2106	
		3.625		A/V	ADP2107	

¹ All limits at temperature extremes are guaranteed via correlation using standard statistical quality control (SQC). Typical values are at $T_A = 25^\circ\text{C}$.

² Guaranteed by design.

³ The ADP2105/ADP2106/ADP2107 line regulation was measured in a servo loop on the automated test equipment that adjusts the feedback voltage to achieve a specific COMP voltage.

⁴ All LX (switch) node characteristics are guaranteed only when the LX1 pin and LX2 pin are tied together.

⁵ These specifications are guaranteed from -40°C to $+85^\circ\text{C}$.

ABSOLUTE MAXIMUM RATINGS

Table 2.

Parameter	Rating
IN, EN, SS, COMP, FB to AGND	-0.3 V to +6 V
LX1, LX2 to PGND	-0.3 V to ($V_{IN} + 0.3$ V)
PWIN1, PWIN2 to PGND	-0.3 V to +6 V
PGND to AGND	-0.3 V to +0.3 V
GND to AGND	-0.3 V to +0.3 V
PWIN1, PWIN2 to IN	-0.3 V to +0.3 V
Operating Junction Temperature Range	-40°C to +125°C
Storage Temperature Range	-65°C to +150°C
Soldering Conditions	JEDEC J-STD-020

Stresses above those listed under Absolute Maximum Ratings may cause permanent damage to the device. This is a stress rating only; functional operation of the device at these or any other conditions above those indicated in the operational section of this specification is not implied. Exposure to absolute maximum rating conditions for extended periods may affect device reliability.

THERMAL RESISTANCE

θ_{JA} is specified for the worst-case conditions, that is, a device soldered in a circuit board for surface-mount packages.

Table 3. Thermal Resistance

Package Type	θ_{JA}	Unit
16-Lead LFCSP_VQ/QFN	40	°C/W
Maximum Power Dissipation	1	W

BOUNDARY CONDITION

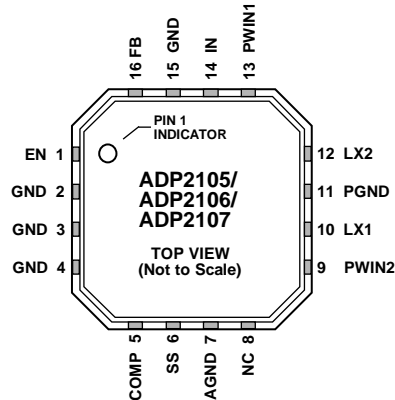
Natural convection, 4-layer board, exposed pad soldered to the PCB.

ESD CAUTION



ESD (electrostatic discharge) sensitive device. Charged devices and circuit boards can discharge without detection. Although this product features patented or proprietary protection circuitry, damage may occur on devices subjected to high energy ESD. Therefore, proper ESD precautions should be taken to avoid performance degradation or loss of functionality.

PIN CONFIGURATION AND FUNCTION DESCRIPTIONS



- NOTES
1. NC = NO CONNECT. DO NOT CONNECT TO THIS PIN.
 2. THE EXPOSED PAD SHOULD BE SOLDERED TO AN EXTERNAL GROUND PLANE UNDERNEATH THE IC FOR THERMAL DISSIPATION.

06079-003

Figure 4. Pin Configuration

Table 4. Pin Function Descriptions

Pin No.	Mnemonic	Description
1	EN	Enable Input. Drive EN high to turn on the device. Drive EN low to turn off the device and reduce the input current to 0.1 μ A.
2, 3, 4, 15	GND	Test Pins. These pins are used for internal testing and are not ground return pins. These pins are to be tied to the AGND plane as close as possible to the ADP2105/ADP2106/ADP2107.
5	COMP	Feedback Loop Compensation Node. COMP is the output of the internal transconductance error amplifier. Place a series RC network from COMP to AGND to compensate the converter. See the Loop Compensation section.
6	SS	Soft Start Input. Place a capacitor from SS to AGND to set the soft start period. A 1 nF capacitor sets a 1 ms soft start period.
7	AGND	Analog Ground. Connect the ground of the compensation components, the soft start capacitor, and the voltage divider on the FB pin to the AGND pin as close as possible to the ADP2105/ADP2106/ADP2107. The AGND is also to be connected to the exposed pad of ADP2105/ADP2106/ADP2107.
8	NC	No Connect. This is not internally connected and can be connected to other pins or left unconnected.
9, 13	PWIN2, PWIN1	Power Source Inputs. The source of the PFET high-side switch. Bypass each PWIN pin to the nearest PGND plane with a 4.7 μ F or greater capacitor as close as possible to the ADP2105/ADP2106/ADP2107. See the Input Capacitor Selection section.
10, 12	LX1, LX2	Switch Outputs. The drain of the P-channel power switch and N-channel synchronous rectifier. These pins are to be tied together and connected to the output LC filter between LX and the output voltage.
11	PGND	Power Ground. Connect the ground return of all input and output capacitors to the PGND pin using a power ground plane as close as possible to the ADP2105/ADP2106/ADP2107. The PGND is then to be connected to the exposed pad of the ADP2105/ADP2106/ADP2107.
14	IN	Power Input. The power source for the ADP2105/ADP2106/ADP2107 internal circuitry. Connect IN and PWIN1 with a 10 Ω resistor as close as possible to the ADP2105/ADP2106/ADP2107. Bypass IN to AGND with a 0.1 μ F or greater capacitor. See the Input Filter section.
16	FB	Output Voltage Sense or Feedback Input. For fixed output versions, connect to the output voltage. For adjustable versions, FB is the input to the error amplifier. Drive FB through a resistive voltage divider to set the output voltage. The FB regulation voltage is 0.8 V.
	EP	Exposed Pad. The exposed pad should be soldered to an external ground plane underneath the IC for thermal dissipation.

TYPICAL PERFORMANCE CHARACTERISTICS

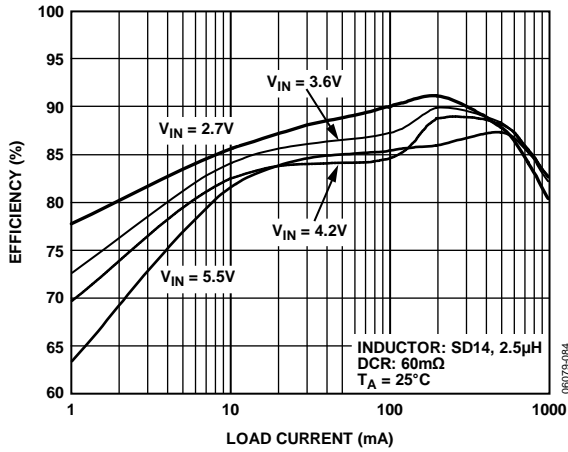


Figure 5. Efficiency—ADP2105 (1.2 V Output)

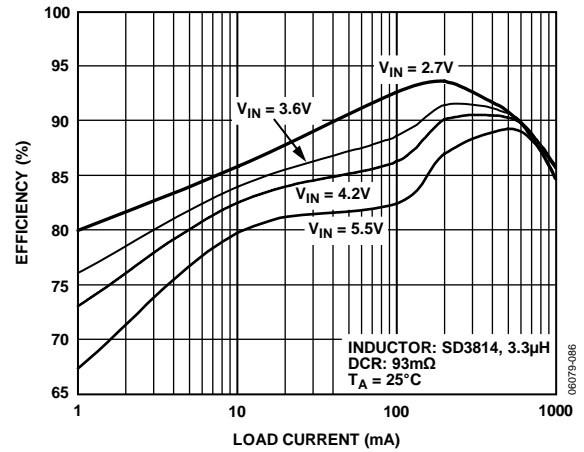


Figure 8. Efficiency—ADP2105 (1.8 V Output)

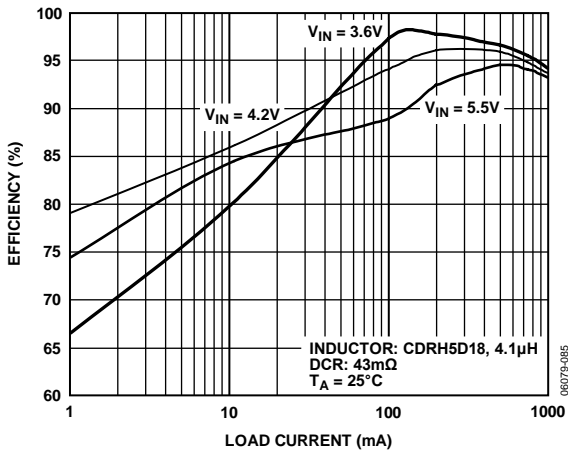


Figure 6. Efficiency—ADP2105 (3.3 V Output)

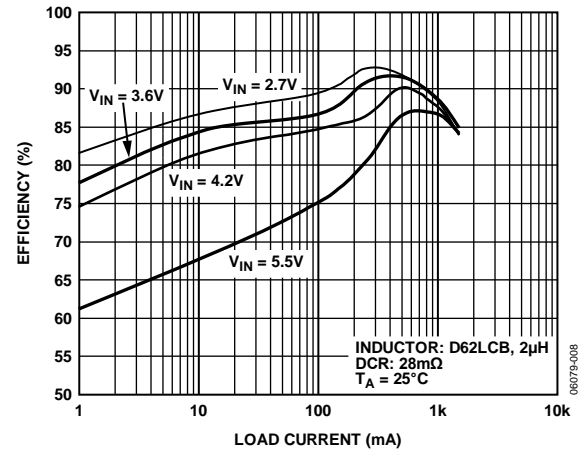


Figure 9. Efficiency—ADP2106 (1.2 V Output)

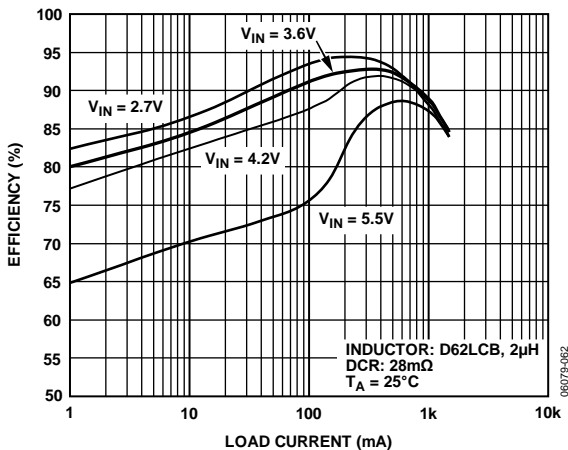


Figure 7. Efficiency—ADP2106 (1.8 V Output)

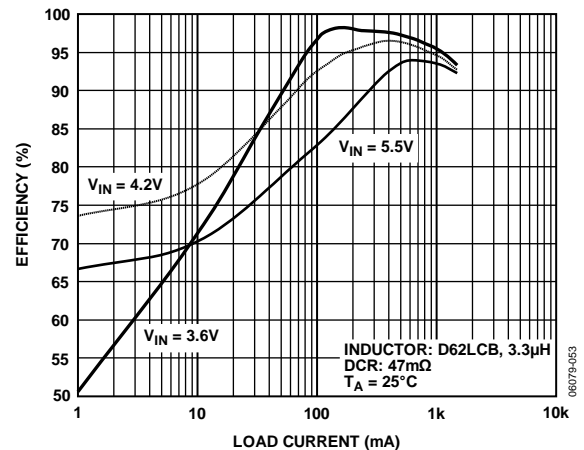


Figure 10. Efficiency—ADP2106 (3.3 V Output)

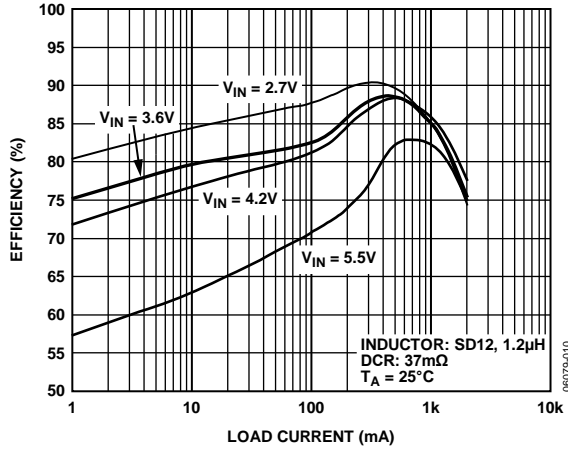


Figure 11. Efficiency—ADP2107 (1.2 V)

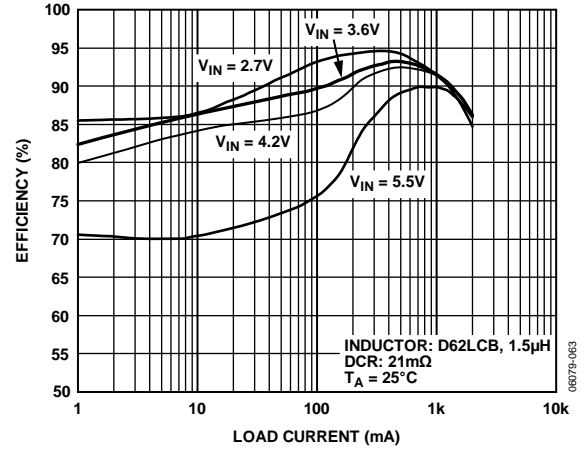


Figure 14. Efficiency—ADP2107 (1.8 V)

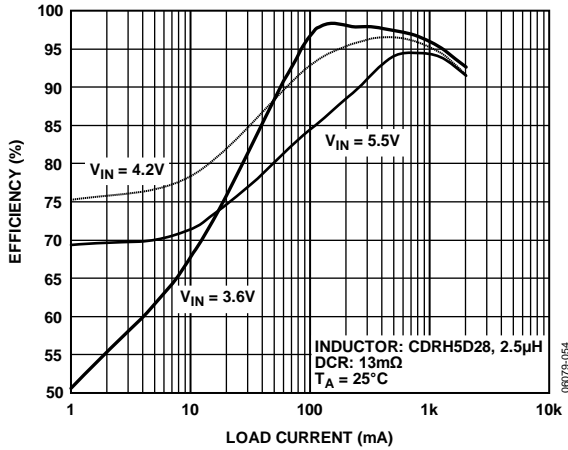


Figure 12. Efficiency—ADP2107 (3.3 V)

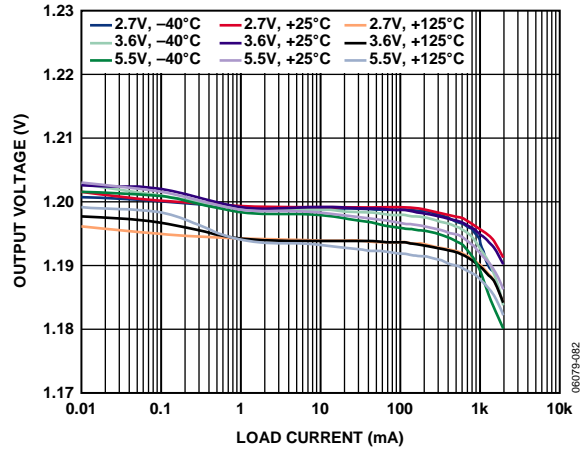


Figure 15. Output Voltage Accuracy—ADP2107 (1.2 V)

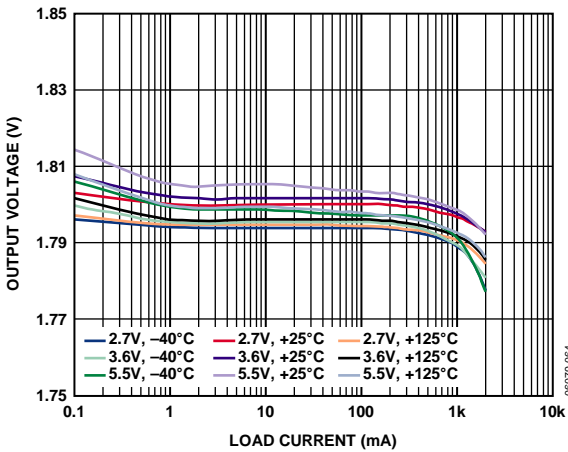


Figure 13. Output Voltage Accuracy—ADP2107 (1.8 V)

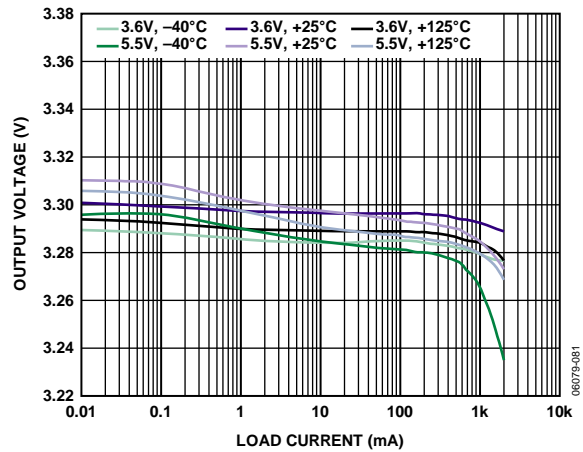


Figure 16. Output Voltage Accuracy—ADP2107 (3.3 V)

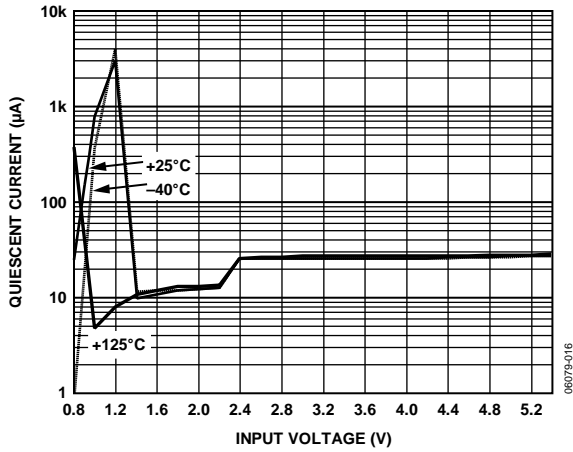


Figure 17. Quiescent Current vs. Input Voltage

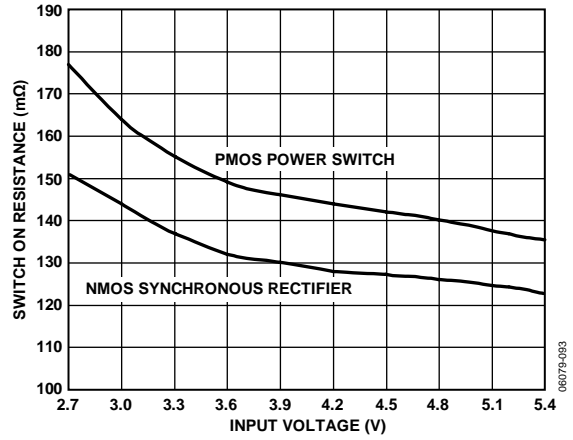


Figure 20. Switch On Resistance vs. Input Voltage—ADP2105

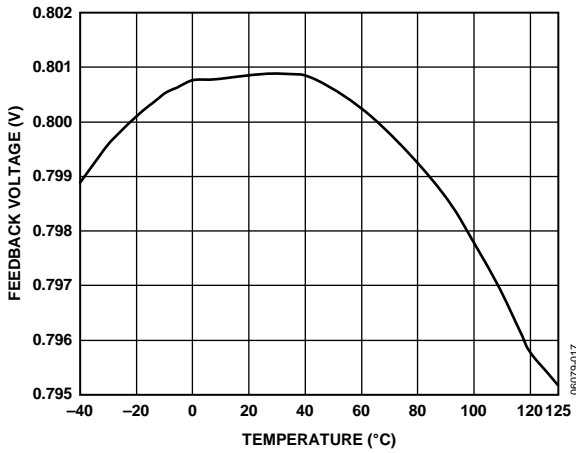


Figure 18. Feedback Voltage vs. Temperature

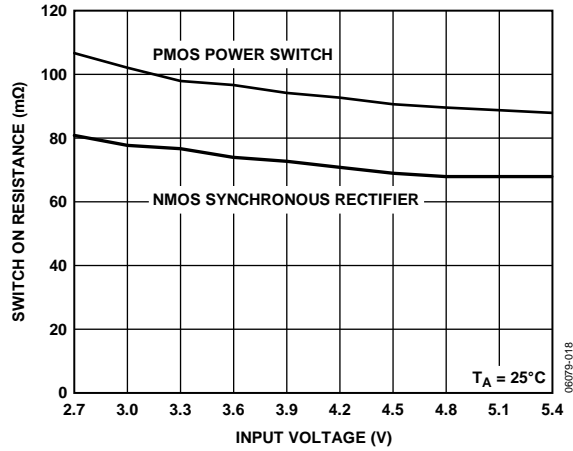


Figure 21. Switch On Resistance vs. Input Voltage—ADP2106 and ADP2107

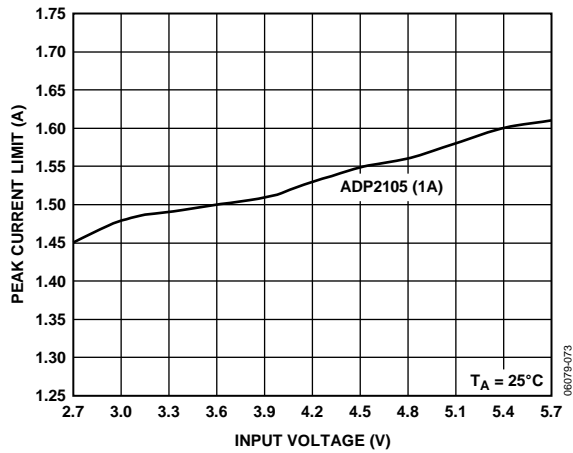


Figure 19. Peak Current Limit of ADP2105

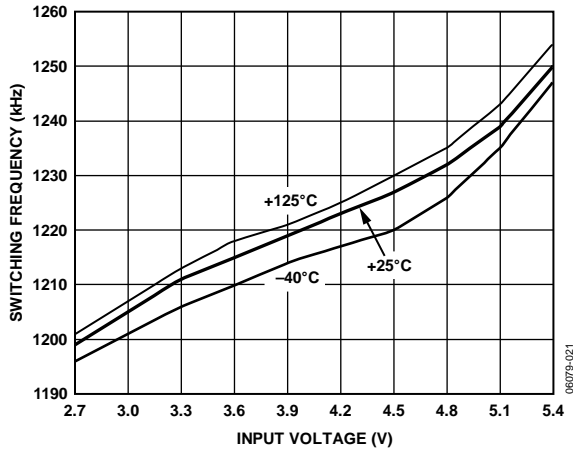


Figure 22. Switching Frequency vs. Input Voltage

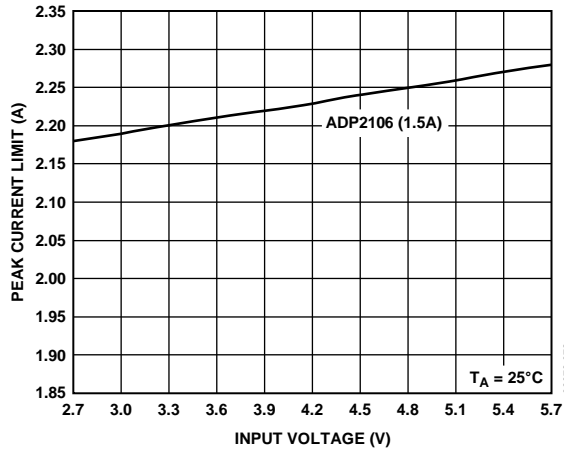


Figure 23. Peak Current Limit of ADP2106

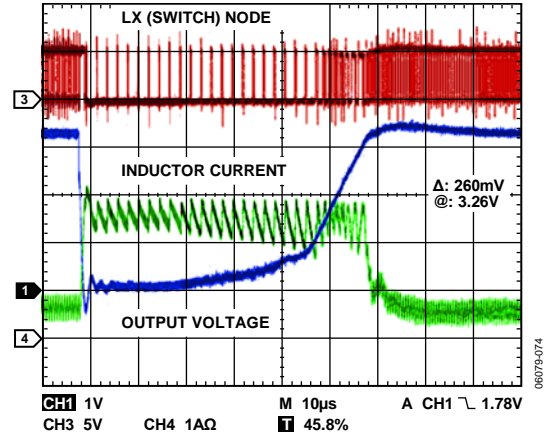


Figure 26. Short-Circuit Response at Output

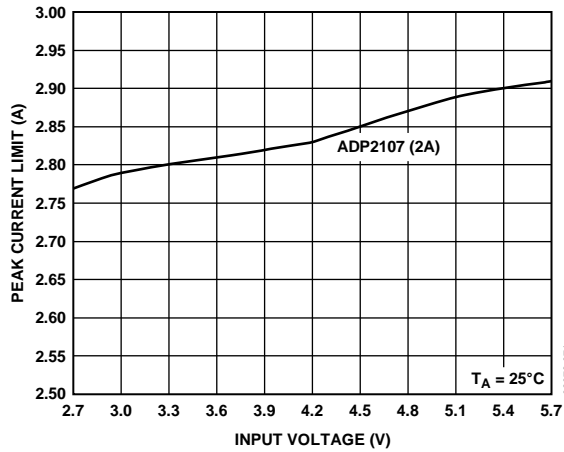


Figure 24. Peak Current Limit of ADP2107

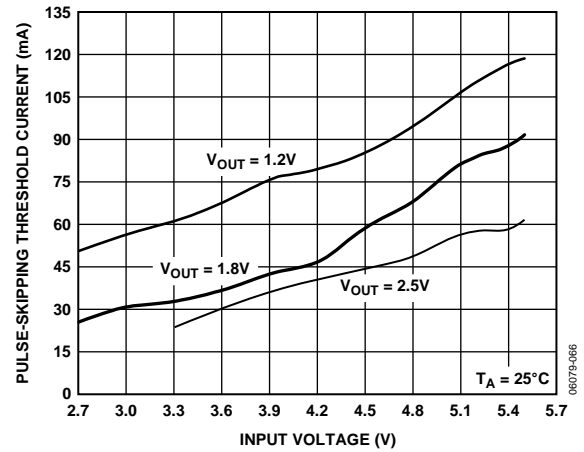


Figure 27. Pulse-Skipping Threshold vs. Input Voltage for ADP2105

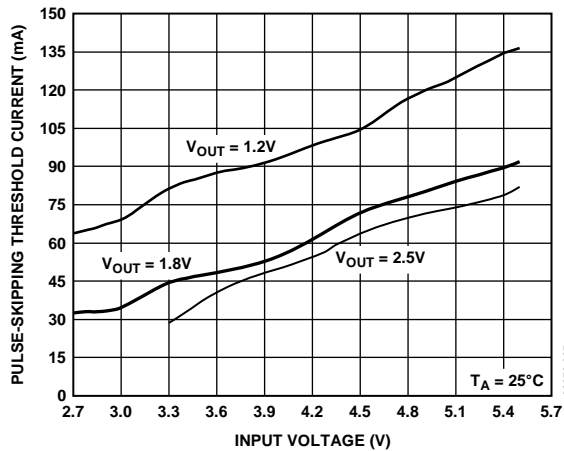


Figure 25. Pulse-Skipping Threshold vs. Input Voltage for ADP2106

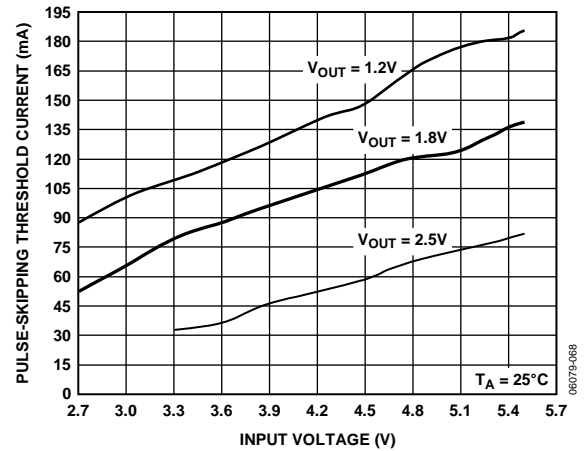


Figure 28. Pulse-Skipping Threshold vs. Input Voltage for ADP2107

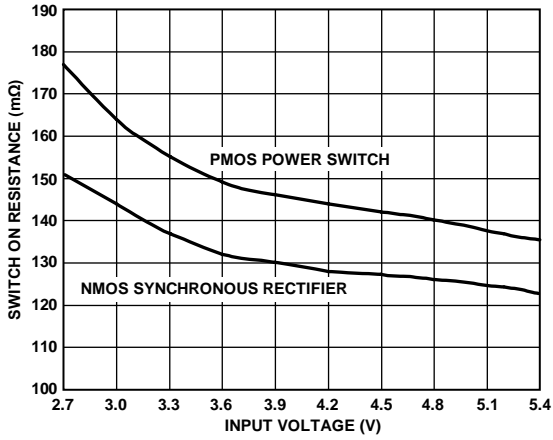


Figure 29. Switch On Resistance vs. Temperature—ADP2105

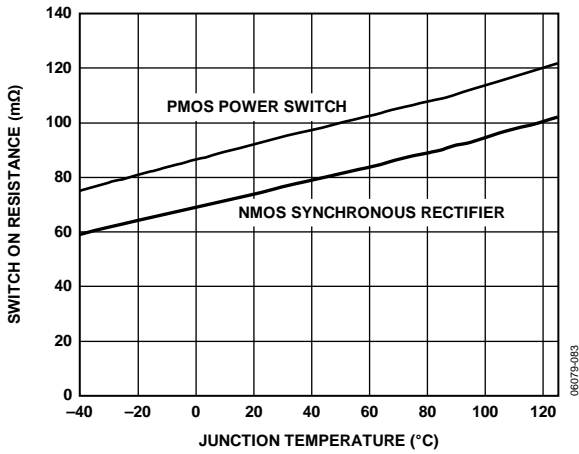


Figure 30. Switch On Resistance vs. Temperature—ADP2106 and ADP2107

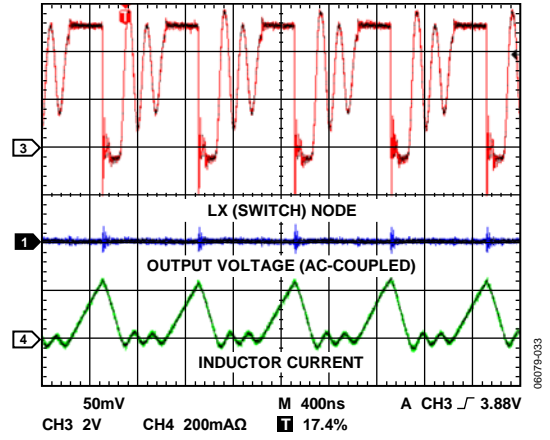


Figure 32. DCM Mode of Operation at Light Load (100 mA)

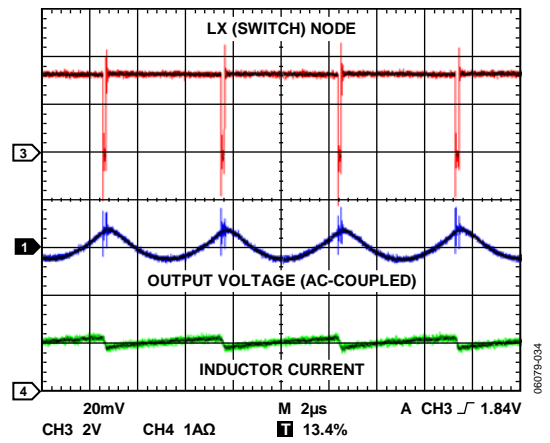


Figure 33. Minimum Off Time Control at Drop

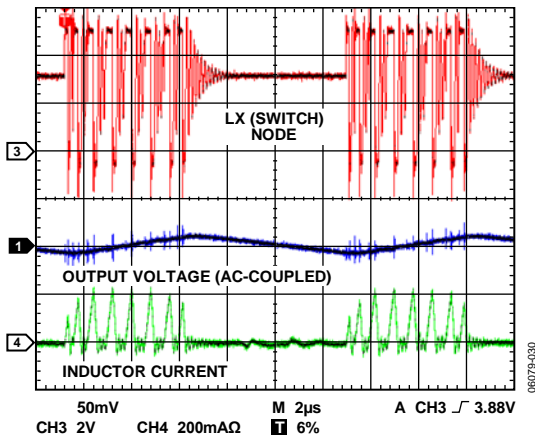


Figure 31. PFM Mode of Operation at Very Light Load (10 mA)

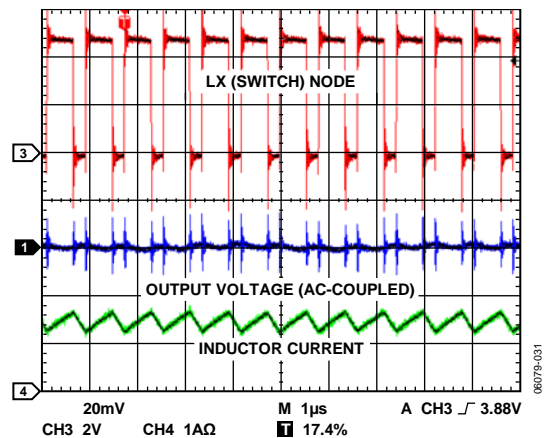


Figure 34. PWM Mode of Operation at Medium/Heavy Load (1.5 A)

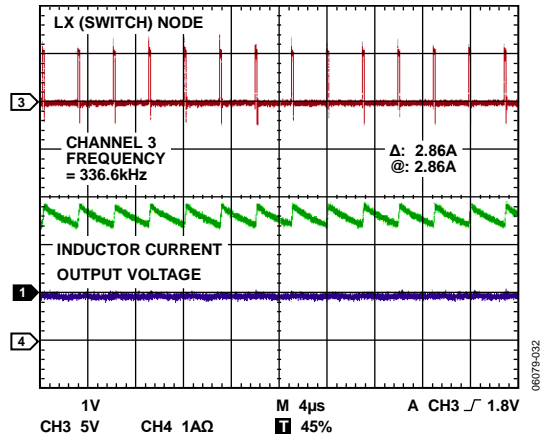


Figure 35. Current Limit Behavior of ADP2107 (Frequency Foldback)

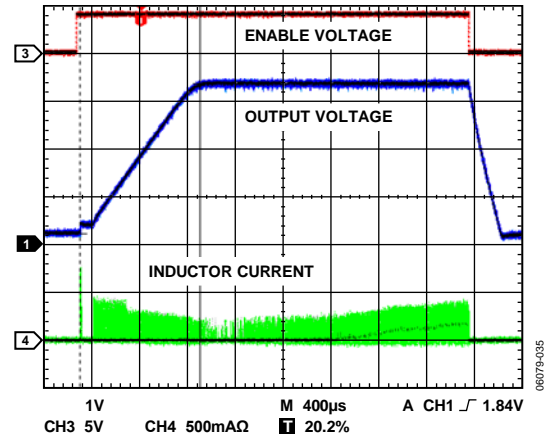


Figure 36. Startup and Shutdown Waveform ($C_{SS} = 1 \text{ nF} \rightarrow \text{SS Time} = 1 \text{ ms}$)

THEORY OF OPERATION

The ADP2105/ADP2106/ADP2107 are step-down, dc-to-dc converters that use a fixed frequency, peak current mode architecture with an integrated high-side switch and low-side synchronous rectifier. The high 1.2 MHz switching frequency and tiny 16-lead, 4 mm × 4 mm LFCSP_VQ package allow for a small step-down dc-to-dc converter solution. The integrated high-side switch (P-channel MOSFET) and synchronous rectifier (N-channel MOSFET) yield high efficiency at medium to heavy loads. Light load efficiency is improved by smoothly transitioning to variable frequency PFM mode.

The ADP2105/ADP2106/ADP2107 (ADJ) operate with an input voltage from 2.7 V to 5.5 V and regulate an output voltage down to 0.8 V. The ADP2105/ADP2106/ADP2107 are also available with preset output voltage options of 3.3 V, 1.8 V, 1.5 V, and 1.2 V.

CONTROL SCHEME

The ADP2105/ADP2106/ADP2107 operate with a fixed frequency, peak current mode PWM control architecture at medium to high loads for high efficiency, but shift to a variable frequency PFM control scheme at light loads for lower quiescent current. When operating in fixed frequency PWM mode, the duty cycle of the integrated switches is adjusted to regulate the output voltage, but when operating in PFM mode at light loads, the switching frequency is adjusted to regulate the output voltage.

The ADP2105/ADP2106/ADP2107 operate in the PWM mode only when the load current is greater than the pulse-skipping threshold current. At load currents below this value, the converter smoothly transitions to the PFM mode of operation.

PWM MODE OPERATION

In PWM mode, the ADP2105/ADP2106/ADP2107 operate at a fixed frequency of 1.2 MHz set by an internal oscillator. At the start of each oscillator cycle, the P-channel MOSFET switch is turned on, putting a positive voltage across the inductor. Current in the inductor increases until the current sense signal crosses the peak inductor current level that turns off the P-channel MOSFET switch and turns on the N-channel MOSFET synchronous rectifier. This puts a negative voltage across the inductor, causing the inductor current to decrease. The synchronous rectifier stays on for the remainder of the cycle, unless the inductor current reaches zero, which causes the zero-crossing comparator to turn off the N-channel MOSFET. The peak inductor current is set by the voltage on the COMP pin. The COMP pin is the output of a transconductance error amplifier that compares the feedback voltage with an internal 0.8 V reference.

PFM MODE OPERATION

The ADP2105/ADP2106/ADP2107 smoothly transition to the variable frequency PFM mode of operation when the load current decreases below the pulse skipping threshold current, switching only as necessary to maintain the output voltage within regulation. When the output voltage dips below regulation, the ADP2105/ADP2106/ADP2107 enter PWM mode for a few oscillator cycles to increase the output voltage back to regulation. During the wait time between bursts, both power switches are off, and the output capacitor supplies all the load current. Because the output voltage dips and recovers occasionally, the output voltage ripple in this mode is larger than the ripple in the PWM mode of operation.

PULSE-SKIPPING THRESHOLD

The output current at which the ADP2105/ADP2106/ADP2107 transition from variable frequency PFM control to fixed frequency PWM control is called the pulse-skipping threshold. The pulse-skipping threshold is optimized for excellent efficiency over all load currents. The variation of pulse-skipping threshold with input voltage and output voltage is shown in Figure 25, Figure 27, and Figure 28.

100% DUTY CYCLE OPERATION (LDO MODE)

As the input voltage drops, approaching the output voltage, the ADP2105/ADP2106/ADP2107 smoothly transition to 100% duty cycle, maintaining the P-channel MOSFET switch-on continuously. This allows the ADP2105/ADP2106/ADP2107 to regulate the output voltage until the drop in input voltage forces the P-channel MOSFET switch to enter dropout, as shown in the following equation:

$$V_{IN(MIN)} = I_{OUT} \times (R_{DS(ON)-P} + DCR_{IND}) + V_{OUT(NOM)}$$

The ADP2105/ADP2106/ADP2107 achieve 100% duty cycle operation by stretching the P-channel MOSFET switch-on time if the inductor current does not reach the peak inductor current level by the end of the clock cycle. When this happens, the oscillator remains off until the inductor current reaches the peak inductor current level, at which time the switch is turned off and the synchronous rectifier is turned on for a fixed off time. At the end of the fixed off time, another cycle is initiated. As the ADP2105/ADP2106/ADP2107 approach dropout, the switching frequency decreases gradually to smoothly transition to 100% duty cycle operation.

SLOPE COMPENSATION

Slope compensation stabilizes the internal current control loop of the ADP2105/ADP2106/ADP2107 when operating beyond 50% duty cycle to prevent subharmonic oscillations. It is implemented by summing a fixed, scaled voltage ramp to the current sense signal during the on-time of the P-channel MOSFET switch.

The slope compensation ramp value determines the minimum inductor that can be used to prevent subharmonic oscillations at a given output voltage. For slope compensation ramp values, see Table 5. For more information see the Inductor Selection section.

Table 5. Slope Compensation Ramp Values

Part	Slope Compensation Ramp Values
ADP2105	0.72 A/μs
ADP2106	1.07 A/μs
ADP2107	1.38 A/μs

DESIGN FEATURES

Enable/Shutdown

Drive EN high to turn on the ADP2105/ADP2106/ADP2107. Drive EN low to turn off the ADP2105/ADP2106/ADP2107, reducing the input current below 0.1 μA. To force the ADP2105/ADP2106/ADP2107 to automatically start when input power is applied, connect EN to IN. When shut down, the ADP2105/ADP2106/ADP2107 discharge the soft start capacitor, causing a new soft start cycle every time they are re-enabled.

Synchronous Rectification

In addition to the P-channel MOSFET switch, the ADP2105/ADP2106/ADP2107 include an integrated N-channel MOSFET synchronous rectifier. The synchronous rectifier improves efficiency, especially at low output voltage, and reduces cost and board space by eliminating the need for an external rectifier.

Current Limit

The ADP2105/ADP2106/ADP2107 have protection circuitry to limit the direction and amount of current flowing through the power switch and synchronous rectifier. The positive current limit on the power switch limits the amount of current that can flow from the input to the output, and the negative current limit on the synchronous rectifier prevents the inductor current from reversing direction and flowing out of the load.

Short-Circuit Protection

The ADP2105/ADP2106/ADP2107 include frequency foldback to prevent output current runaway on a hard short. When the voltage at the feedback pin falls below 0.3 V, indicating the possibility of a hard short at the output, the switching frequency is reduced to 1/4 of the internal oscillator frequency. The reduction in the switching frequency results in more time for the inductor to discharge, preventing a runaway of output current.

Undervoltage Lockout (UVLO)

To protect against deep battery discharge, UVLO circuitry is integrated on the ADP2105/ADP2106/ADP2107. If the input voltage drops below the 2.2 V UVLO threshold, the ADP2105/ADP2106/ADP2107 shut down, and both the power switch and synchronous rectifier turn off. When the voltage again rises above the UVLO threshold, the soft start period is initiated, and the part is enabled.

Thermal Protection

In the event that the ADP2105/ADP2106/ADP2107 junction temperatures rise above 140°C, the thermal shutdown circuit turns off the converter. Extreme junction temperatures can be the result of high current operation, poor circuit board design, and/or high ambient temperature. A 40°C hysteresis is included so that when thermal shutdown occurs, the ADP2105/ADP2106/ADP2107 do not return to operation until the on-chip temperature drops below 100°C. When coming out of thermal shutdown, soft start is initiated.

Soft Start

The ADP2105/ADP2106/ADP2107 include soft start circuitry to limit the output voltage rise time to reduce inrush current at startup. To set the soft start period, connect the soft start capacitor (C_{SS}) from SS to AGND. When the ADP2105/ADP2106/ADP2107 are disabled, or if the input voltage is below the undervoltage lockout threshold, C_{SS} is internally discharged. When the ADP2105/ADP2106/ADP2107 are enabled, C_{SS} is charged through an internal 0.8 μA current source, causing the voltage at SS to rise linearly. The output voltage rises linearly with the voltage at SS.

APPLICATIONS INFORMATION

ADIsimPower DESIGN TOOL

The ADP2105/ADP2106/ADP2107 is supported by ADIsimPower design tool set. ADIsimPower is a collection of tools that produce complete power designs optimized for a specific design goal. The tools enable the user to generate a full schematic, bill of materials, and calculate performance in minutes. ADIsimPower can optimize designs for cost, area, efficiency, and parts count while taking into consideration the operating conditions and limitations of the IC and all real external components. For more information about ADIsimPower design tools, refer to www.analog.com/ADIsimPower. The tool set is available from this website, and users can also request an unpopulated board through the tool.

EXTERNAL COMPONENT SELECTION

The external component selection for the ADP2105/ADP2106/ADP2107 application circuits shown in Figure 37 and Figure 38 depend on input voltage, output voltage, and load current requirements. Additionally, trade-offs between performance parameters like efficiency and transient response can be made by varying the choice of external components.

SETTING THE OUTPUT VOLTAGE

The output voltage of ADP2105/ADP2106/ADP2107(ADJ) is externally set by a resistive voltage divider from the output voltage to FB. The ratio of the resistive voltage divider sets the output voltage, and the absolute value of those resistors sets the divider string current. For lower divider string currents, the small 10 nA (0.1 μA maximum) FB bias current is to be taken into account when calculating resistor values. The FB bias current can be ignored for a higher divider string current, but this degrades efficiency at very light loads.

To limit output voltage accuracy degradation due to FB bias current to less than 0.05% (0.5% maximum), ensure that the divider string current is greater than 20 μA. To calculate the desired resistor values, first determine the value of the bottom divider string resistor (R_{BOT}) using the following equation:

$$R_{BOT} = \frac{V_{FB}}{I_{STRING}}$$

where:

$V_{FB} = 0.8$ V, the internal reference.

I_{STRING} is the resistor divider string current.

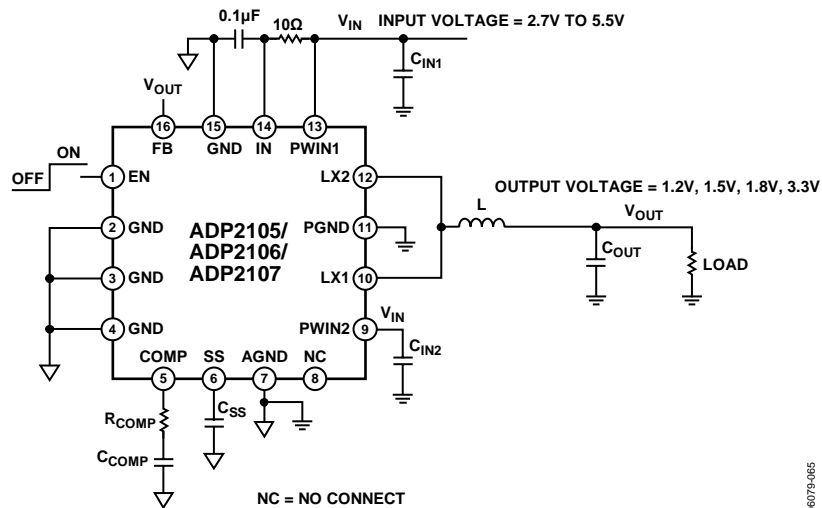


Figure 37. Typical Applications Circuit for Fixed Output Voltage Options of ADP2105/ADP2106/ADP2107(x.x V)

Table 8. Minimum Inductor Value for Common Output Voltage Options for the ADP2107 (2 A)

V _{OUT}	V _{IN}			
	2.7 V	3.6 V	4.2 V	5.5 V
1.2 V	0.83 μH	1.00 μH	1.07 μH	1.17 μH
1.5 V	0.99 μH	1.09 μH	1.21 μH	1.36 μH
1.8 V	1.19 μH	1.19 μH	1.29 μH	1.51 μH
2.5 V	1.65 μH	1.65 μH	1.65 μH	1.70 μH
3.3 V	2.18 μH	2.18 μH	2.18 μH	2.18 μH

Table 9. Inductor Recommendations for the ADP2105/ADP2106/ADP2107

Vendor	Small-Sized Inductors (< 5 mm × 5 mm)	Large-Sized Inductors (> 5 mm × 5 mm)
Sumida	CDRH2D14, 3D16, 3D28	CDRH4D18, 4D22, 4D28, 5D18, 6D12
Toko	1069AS-DB3018, 1098AS-DE2812, 1070AS-DB3020	D52LC, D518LC, D62LCB
Coilcraft	LPS3015, LPS4012, DO3314	DO1605T
Cooper Bussmann	SD3110, SD3112, SD3114, SD3118, SD3812, SD3814	SD10, SD12, SD14, SD52

OUTPUT CAPACITOR SELECTION

The output capacitor selection affects both the output voltage ripple and the loop dynamics of the converter. For a given loop crossover frequency (the frequency at which the loop gain drops to 0 dB), the maximum voltage transient excursion (overshoot) is inversely proportional to the value of the output capacitor. Therefore, larger output capacitors result in improved load transient response. To minimize the effects of the dc-to-dc converter switching, the crossover frequency of the compensation loop should be less than 1/10 of the switching frequency. Higher crossover frequency leads to faster settling time for a load transient response, but it can also cause ringing due to poor phase margin. Lower crossover frequency helps to provide stable operation but needs large output capacitors to achieve competitive overshoot specifications. Therefore, the optimal crossover frequency for the control loop of ADP2105/ADP2106/ADP2107 is 80 kHz, 1/15 of the switching frequency. For a crossover frequency of 80 kHz, Figure 39 shows the maximum output voltage excursion during a 1 A load transient, as the product of the output voltage and the output capacitor is varied. Choose the output capacitor based on the desired load transient response and target output voltage.

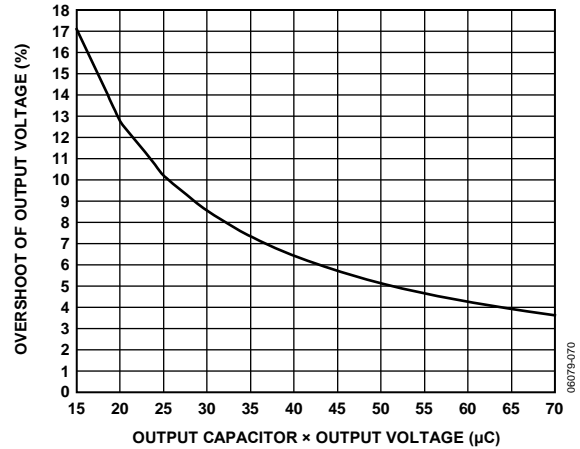


Figure 39. Percentage Overshoot for a 1 A Load Transient Response vs. Output Capacitor × Output Voltage

For example, if the desired 1 A load transient response (overshoot) is 5% for an output voltage of 2.5 V, then from Figure 39

$$\begin{aligned} \text{Output Capacitor} \times \text{Output Voltage} &= 50 \mu\text{C} \\ \Rightarrow \text{Output Capacitor} &= \frac{50 \mu\text{C}}{2.5} \approx 20 \mu\text{F} \end{aligned}$$

The ADP2105/ADP2106/ADP2107 have been designed for operation with small ceramic output capacitors that have low ESR and ESL. Therefore, they are comfortably able to meet tight output voltage ripple specifications. X5R or X7R dielectrics are recommended with a voltage rating of 6.3 V or 10 V. Y5V and Z5U dielectrics are not recommended, due to their poor temperature and dc bias characteristics. Table 10 shows a list of recommended MLCC capacitors from Murata and Taiyo Yuden.

When choosing output capacitors, it is also important to account for the loss of capacitance due to output voltage dc bias. Figure 40 shows the loss of capacitance due to output voltage dc bias for three X5R MLCC capacitors from Murata.

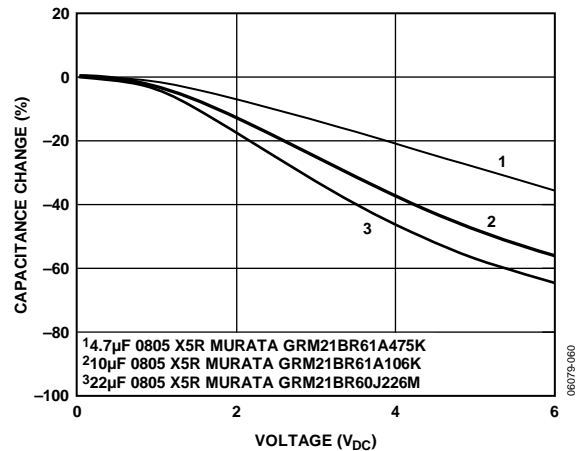


Figure 40. Percentage Drop-In Capacitance vs. DC Bias for Ceramic Capacitors (Information Provided by Murata Corporation)

For example, to get 20 μF output capacitance at an output voltage of 2.5 V, based on Figure 40, as well as to give some margin for temperature variance, a 22 μF and a 10 μF capacitor are to be

used in parallel to ensure that the output capacitance is sufficient under all conditions for stable behavior.

Table 10. Recommended Input and Output Capacitor Selection for the ADP2105/ADP2106/ADP2107

Capacitor	Vendor	
	Murata	Taiyo Yuden
4.7 μ F, 10 V X5R 0805	GRM21BR61A475K	LMK212BJ475KG
10 μ F, 10 V X5R 0805	GRM21BR61A106K	LMK212BJ106KG
22 μ F, 6.3 V X5R 0805	GRM21BR60J226M	JMK212BJ226MG

INPUT CAPACITOR SELECTION

The input capacitor reduces input voltage ripple caused by the switch currents on the PWIN pins. Place the input capacitors as close as possible to the PWIN pins. Select an input capacitor capable of withstanding the rms input current for the maximum load current in your application.

For the ADP2105, it is recommended that each PWIN pin be bypassed with a 4.7 μ F or larger input capacitor. For the ADP2106, bypass each PWIN pin with a 10 μ F and a 4.7 μ F capacitor, and for the ADP2107, bypass each PWIN pin with a 10 μ F capacitor.

As with the output capacitor, a low ESR ceramic capacitor is recommended to minimize input voltage ripple. X5R or X7R dielectrics are recommended, with a voltage rating of 6.3 V or 10 V. Y5V and Z5U dielectrics are not recommended due to their poor temperature and dc bias characteristics. Refer to Table 10 for input capacitor recommendations.

INPUT FILTER

The IN pin is the power source for the ADP2105/ADP2106/ADP2107 internal circuitry, including the voltage reference and current sense amplifier that are sensitive to power supply noise. To prevent high frequency switching noise on the PWIN pins from corrupting the internal circuitry of the ADP2105/ADP2106/ADP2107, a low-pass RC filter should be placed between the IN pin and the PWIN1 pin. The suggested input filter consists of a small 0.1 μ F ceramic capacitor placed between IN and AGND and a 10 Ω resistor placed between IN and PWIN1. This forms a 150 kHz low-pass filter between PWIN1 and IN that prevents any high frequency noise on PWIN1 from coupling into the IN pin.

SOFT START PERIOD

To set the soft start period, connect a soft start capacitor (C_{SS}) from SS to AGND. The soft start period varies linearly with the size of the soft start capacitor, as shown in the following equation:

$$T_{SS} = C_{SS} \times 10^9 \text{ ms}$$

For a soft start period of 1 ms, a 1 nF capacitor must be connected between SS and AGND.

LOOP COMPENSATION

The ADP2105/ADP2106/ADP2107 utilize a transconductance error amplifier to compensate the external voltage loop. The open loop transfer function at angular frequency (s) is given by

$$H(s) = G_m G_{CS} \left(\frac{Z_{COMP}(s)}{s C_{OUT}} \right) \left(\frac{V_{REF}}{V_{OUT}} \right)$$

where:

V_{REF} is the internal reference voltage (0.8 V).

V_{OUT} is the nominal output voltage.

$Z_{COMP}(s)$ is the impedance of the compensation network at the angular frequency.

C_{OUT} is the output capacitor.

g_m is the transconductance of the error amplifier (50 μ A/V nominal).

G_{CS} is the effective transconductance of the current loop.

$$G_{CS} = 1.875 \text{ A/V for the ADP2105.}$$

$$G_{CS} = 2.8125 \text{ A/V for the ADP2106.}$$

$$G_{CS} = 3.625 \text{ A/V for the ADP2107.}$$

The transconductance error amplifier drives the compensation network that consists of a resistor (R_{COMP}) and capacitor (C_{COMP}) connected in series to form a pole and a zero, as shown in the following equation:

$$Z_{COMP}(s) = \left(R_{COMP} + \frac{1}{s C_{COMP}} \right) = \left(\frac{1 + s R_{COMP} C_{COMP}}{s C_{COMP}} \right)$$

At the crossover frequency, the gain of the open loop transfer function is unity. For the compensation network impedance at the crossover frequency, this yields the following equation:

$$Z_{COMP}(F_{CROSS}) = \left(\frac{(2\pi) F_{CROSS}}{G_m G_{CS}} \right) \left(\frac{C_{OUT} V_{OUT}}{V_{REF}} \right)$$

where:

$F_{CROSS} = 80 \text{ kHz}$, the crossover frequency of the loop.

$C_{OUT} V_{OUT}$ is determined from the Output Capacitor Selection section.

To ensure that there is sufficient phase margin at the crossover frequency, place the compensator zero at 1/4 of the crossover frequency, as shown in the following equation:

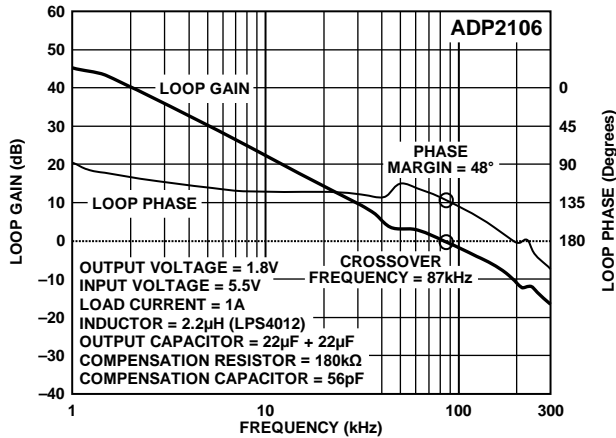
$$(2\pi) \left(\frac{F_{CROSS}}{4} \right) R_{COMP} C_{COMP} = 1$$

Solving the three equations in this section simultaneously yields the value for the compensation resistor and compensation capacitor, as shown in the following equation:

$$R_{COMP} = 0.8 \left(\frac{(2\pi) F_{CROSS}}{G_m G_{CS}} \right) \left(\frac{C_{OUT} V_{OUT}}{V_{REF}} \right)$$

$$C_{COMP} = \frac{2}{\pi F_{CROSS} R_{COMP}}$$

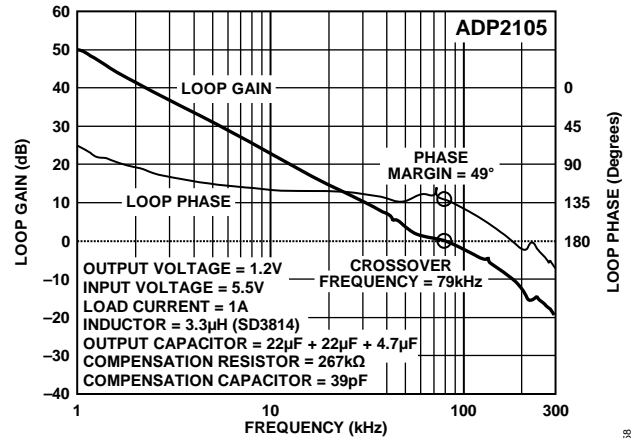
BODE PLOTS



NOTES
 1. EXTERNAL COMPONENTS WERE CHOSEN FOR A 5% OVERSHOOT FOR A 1A LOAD TRANSIENT.

06079-055

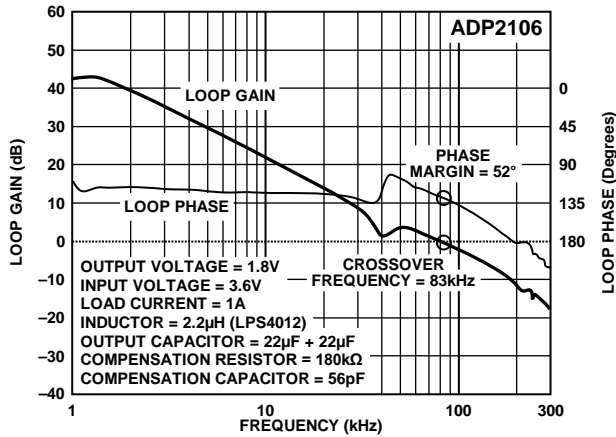
Figure 41. ADP2106 Bode Plot at $V_{IN} = 5.5V$, $V_{OUT} = 1.8V$ and Load = 1 A



NOTES
 1. EXTERNAL COMPONENTS WERE CHOSEN FOR A 5% OVERSHOOT FOR A 1A LOAD TRANSIENT.

06079-058

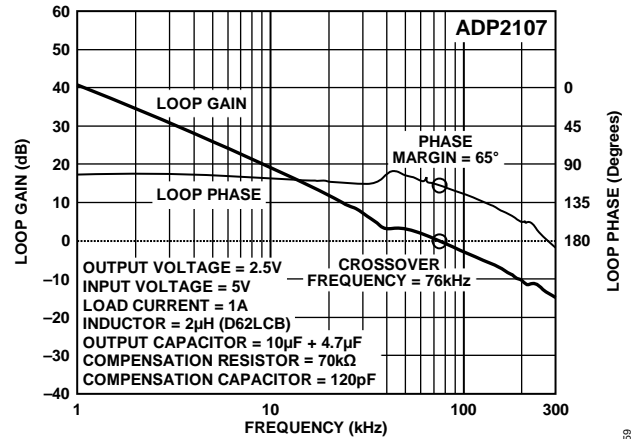
Figure 44. ADP2105 Bode Plot at $V_{IN} = 5.5V$, $V_{OUT} = 1.2V$ and Load = 1 A



NOTES
 1. EXTERNAL COMPONENTS WERE CHOSEN FOR A 5% OVERSHOOT FOR A 1A LOAD TRANSIENT.

06079-056

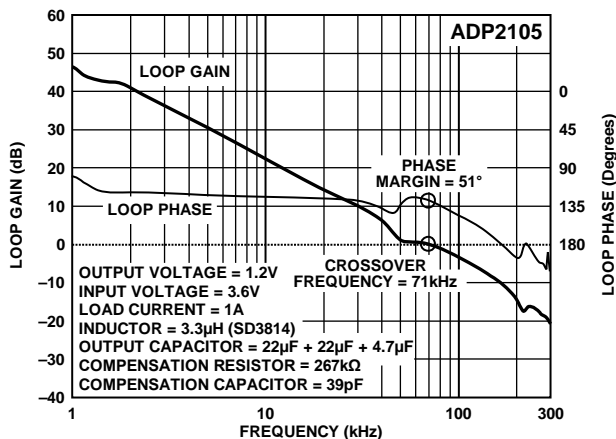
Figure 42. ADP2106 Bode Plot at $V_{IN} = 3.6V$, $V_{OUT} = 1.8V$, and Load = 1 A



NOTES
 1. EXTERNAL COMPONENTS WERE CHOSEN FOR A 10% OVERSHOOT FOR A 1A LOAD TRANSIENT.

06079-059

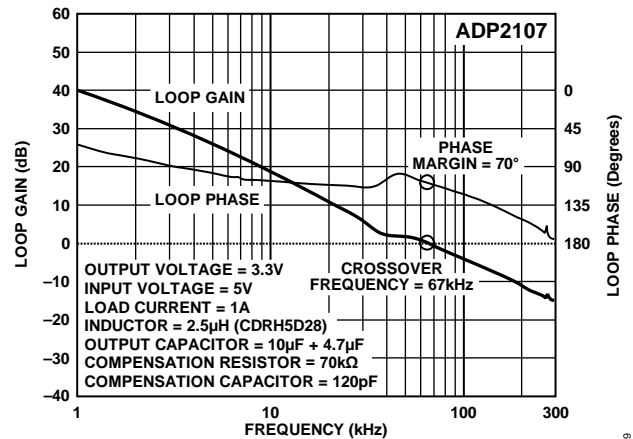
Figure 45. ADP2107 Bode Plot at $V_{IN} = 5V$, $V_{OUT} = 2.5V$ and Load = 1 A



NOTES
 1. EXTERNAL COMPONENTS WERE CHOSEN FOR A 5% OVERSHOOT FOR A 1A LOAD TRANSIENT.

06079-057

Figure 43. ADP2105 Bode Plot at $V_{IN} = 3.6V$, $V_{OUT} = 1.2V$, and Load = 1 A



NOTES
 1. EXTERNAL COMPONENTS WERE CHOSEN FOR A 10% OVERSHOOT FOR A 1A LOAD TRANSIENT.

06079-069

Figure 46. ADP2107 Bode Plot at $V_{IN} = 5V$, $V_{OUT} = 3.3V$, and Load = 1 A

LOAD TRANSIENT RESPONSE

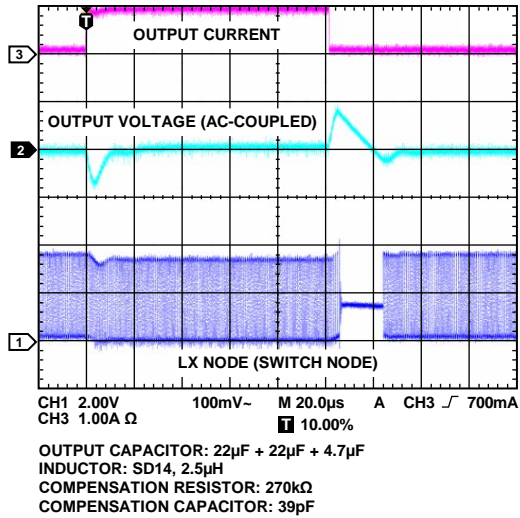


Figure 47. 1 A Load Transient Response for ADP2105-1.2 with External Components Chosen for 5% Overshoot

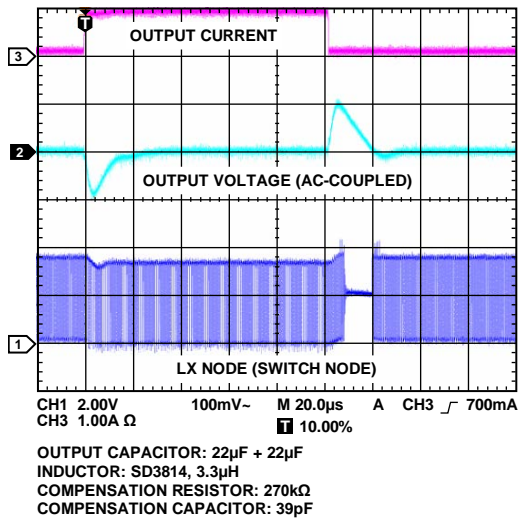


Figure 48. 1 A Load Transient Response for ADP2105-1.8 with External Components Chosen for 5% Overshoot

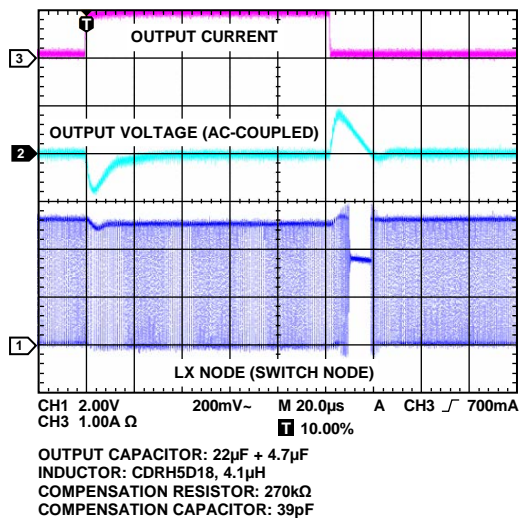


Figure 49. 1 A Load Transient Response for ADP2105-3.3 with External Components Chosen for 5% Overshoot

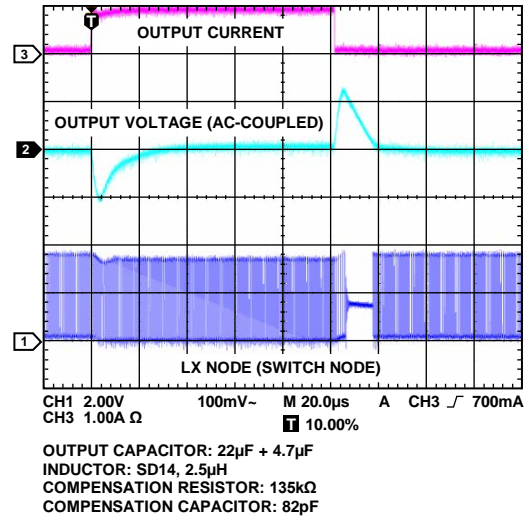


Figure 50. 1 A Load Transient Response for ADP2105-1.2 with External Components Chosen for 10% Overshoot

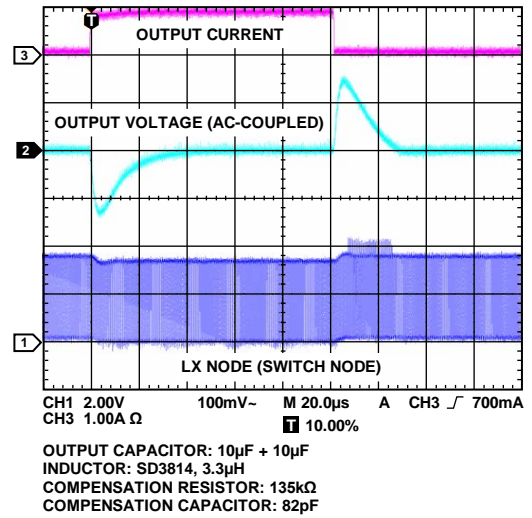


Figure 51. 1 A Load Transient Response for ADP2105-1.8 with External Components Chosen for 10% Overshoot

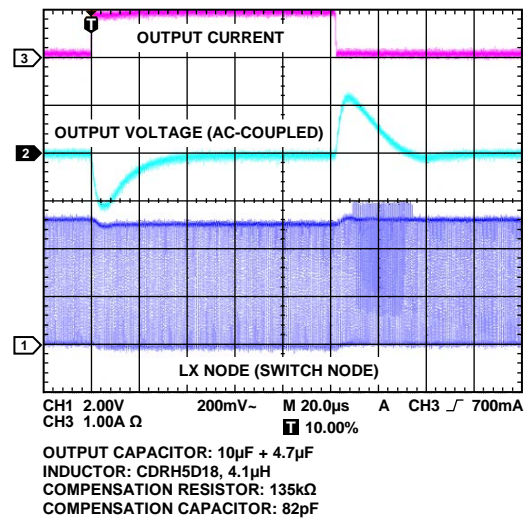


Figure 52. 1 A Load Transient Response for ADP2105-3.3 with External Components Chosen for 10% Overshoot

EFFICIENCY CONSIDERATIONS

Efficiency is the ratio of output power to input power. The high efficiency of the ADP2105/ADP2106/ADP2107 has two distinct advantages. First, only a small amount of power is lost in the dc-to-dc converter package that reduces thermal constraints. Second, the high efficiency delivers the maximum output power for the given input power, extending battery life in portable applications.

There are four major sources of power loss in dc-to-dc converters like the ADP2105/ADP2106/ADP2107:

- Power switch conduction losses
- Inductor losses
- Switching losses
- Transition losses

Power Switch Conduction Losses

Power switch conduction losses are caused by the flow of output current through the P-channel power switch and the N-channel synchronous rectifier, which have internal resistances ($R_{DS(ON)}$) associated with them. The amount of power loss can be approximated by

$$P_{SW-COND} = [R_{DS(ON)-P} \times D + R_{DS(ON)-N} \times (1 - D)] \times I_{OUT}^2$$

where $D = V_{OUT}/V_{IN}$.

The internal resistance of the power switches increases with temperature but decreases with higher input voltage. Figure 20 and Figure 21 show the change in $R_{DS(ON)}$ vs. input voltage, whereas Figure 29 and Figure 30 show the change in $R_{DS(ON)}$ vs. temperature for both power devices.

Inductor Losses

Inductor conduction losses are caused by the flow of current through the inductor, which has an internal resistance (DCR) associated with it. Larger sized inductors have smaller DCR, which can improve inductor conduction losses.

Inductor core losses are related to the magnetic permeability of the core material. Because the ADP2105/ADP2106/ADP2107 are high switching frequency dc-to-dc converters, shielded ferrite core material is recommended for its low core losses and low EMI.

The total amount of inductor power loss can be calculated by

$$P_L = DCR \times I_{OUT}^2 + \text{Core Losses}$$

Switching Losses

Switching losses are associated with the current drawn by the driver to turn on and turn off the power devices at the switching frequency. Each time a power device gate is turned on and turned off, the driver transfers a charge ΔQ from the input supply to the gate and then from the gate to ground.

The amount of power loss can be calculated by

$$P_{SW} = (C_{GATE-P} + C_{GATE-N}) \times V_{IN}^2 \times f_{SW}$$

where:

$$(C_{GATE-P} + C_{GATE-N}) \approx 600 \text{ pF}$$

$$f_{SW} = 1.2 \text{ MHz, the switching frequency.}$$

Transition Losses

Transition losses occur because the P-channel MOSFET power switch cannot turn on or turn off instantaneously. At the middle of an LX (switch) node transition, the power switch is providing all the inductor current, while the source to drain voltage of the power switch is half the input voltage, resulting in power loss. Transition losses increase with load current and input voltage and occur twice for each switching cycle.

The amount of power loss can be calculated by

$$P_{TRAN} = \frac{V_{IN}}{2} \times I_{OUT} \times (t_{ON} + t_{OFF}) \times f_{SW}$$

where t_{ON} and t_{OFF} are the rise time and fall time of the LX (switch) node, and are both approximately 3 ns.

THERMAL CONSIDERATIONS

In most applications, the ADP2105/ADP2106/ADP2107 do not dissipate a lot of heat due to their high efficiency. However, in applications with high ambient temperature, low supply voltage, and high duty cycle, the heat dissipated in the package is large enough that it can cause the junction temperature of the die to exceed the maximum junction temperature of 125°C. Once the junction temperature exceeds 140°C, the converter goes into thermal shutdown. To prevent any permanent damage it recovers only after the junction temperature has decreased below 100°C. Therefore, thermal analysis for the chosen application solution is very important to guarantee reliable performance over all conditions.

The junction temperature of the die is the sum of the ambient temperature of the environment and the temperature rise of the package due to the power dissipation, as shown in the following equation:

$$T_J = T_A + T_R$$

where:

T_J is the junction temperature.

T_A is the ambient temperature.

T_R is the rise in temperature of the package due to the power dissipation in the package.

The rise in temperature of the package is directly proportional to the power dissipation in the package. The proportionality constant for this relationship is defined as the thermal resistance from the junction of the die to the ambient temperature, as shown in the following equation:

$$T_R = \theta_{JA} \times P_D$$

where:

T_R is the rise in temperature of the package.

P_D is the power dissipation in the package.

θ_{JA} is the thermal resistance from the junction of the die to the ambient temperature of the package.

For example, in an application where the ADP2107(1.8 V) is used with an input voltage of 3.6 V, a load current of 2 A, and a maximum ambient temperature of 85°C, at a load current of 2 A, the most significant contributor of power dissipation in the dc-to-dc converter package is the conduction loss of the power switches. Using the graph of switch on resistance vs. temperature (see Figure 30), as well as the equation of power loss given in the Power Switch Conduction Losses section, the power dissipation in the package can be calculated by the following:

$$P_{SW-COND} = [R_{DS(ON)-P} \times D + R_{DS(ON)-N} \times (1 - D)] \times I_{OUT}^2 =$$

$$[109 \text{ m}\Omega \times 0.5 + 90 \text{ m}\Omega \times 0.5] \times (2 \text{ A})^2 \approx 400 \text{ mW}$$

The θ_{JA} for the LFCSP_VQ package is 40°C/W, as shown in Table 3. Therefore, the rise in temperature of the package due to power dissipation is

$$T_R = \theta_{JA} \times P_D = 40^\circ\text{C/W} \times 0.40 \text{ W} = 16^\circ\text{C}$$

The junction temperature of the converter is

$$T_J = T_A + T_R = 85^\circ\text{C} + 16^\circ\text{C} = 101^\circ\text{C}$$

Because the junction temperature of the converter is below the maximum junction temperature of 125°C, this application operates reliably from a thermal point of view.

DESIGN EXAMPLE

Consider an application with the following specifications:

Input Voltage = 3.6 V to 4.2 V.

Output Voltage = 2 V.

Typical Output Current = 600 mA.

Maximum Output Current = 1.2 A.

Soft Start Time = 2 ms.

Overshoot \leq 100 mV under all load transient conditions.

1. Choose the dc-to-dc converter that satisfies the maximum output current requirement. Because the maximum output current for this application is 1.2 A, the ADP2106 with a maximum output current of 1.5 A is ideal for this application.
2. See whether the output voltage desired is available as a fixed output voltage option. Because 2 V is not one of the fixed output voltage options available, choose the adjustable version of ADP2106.
3. The first step in external component selection for an adjustable version converter is to calculate the resistance of the resistive voltage divider that sets the output voltage.

$$R_{BOT} = \frac{V_{FB}}{I_{STRING}} = \frac{0.8 \text{ V}}{20 \mu\text{A}} = 40 \text{ k}\Omega$$

$$R_{TOP} = R_{BOT} \left[\frac{V_{OUT} - V_{FB}}{V_{FB}} \right] = 40 \text{ k}\Omega \times \left[\frac{2 \text{ V} - 0.8 \text{ V}}{0.8 \text{ V}} \right] = 60 \text{ k}\Omega$$

Calculate the minimum inductor value as follows:

For the ADP2106:

$$L > (0.83 \mu\text{H/V}) \times V_{OUT}$$

$$\Rightarrow L > 0.83 \mu\text{H/V} \times 2 \text{ V}$$

$$\Rightarrow L > 1.66 \mu\text{H}$$

Next, calculate the ideal inductor value that sets the inductor peak-to-peak current ripple (ΔI_L) to 1/3 of the maximum load current at the maximum input voltage as follows:

$$L_{IDEAL} = \frac{2.5 \times V_{OUT} \times (V_{IN} - V_{OUT})}{V_{IN} \times I_{LOAD(MAX)}} \mu\text{H} =$$

$$\frac{2.5 \times 2 \times (4.2 - 2)}{4.2 \times 1.2} \mu\text{H} = 2.18 \mu\text{H}$$

4. The closest standard inductor value is 2.2 μH . The maximum rms current of the inductor is to be greater than 1.2 A, and the saturation current of the inductor is to be greater than 2 A. One inductor that meets these criteria is the LPS4012-2.2 μH from Coilcraft.
5. Choose the output capacitor based on the transient response requirements. The worst-case load transient is 1.2 A, for which the overshoot must be less than 100 mV, which is 5% of the output voltage. For a 1 A load transient, the overshoot must be less than 4% of the output voltage, then from Figure 39:

$$\text{Output Capacitor} \times \text{Output Voltage} = 60 \mu\text{C}$$

$$\Rightarrow \text{Output Capacitor} = \frac{60 \mu\text{C}}{2.0 \text{ V}} \approx 30 \mu\text{F}$$

Taking into account the loss of capacitance due to dc bias, as shown in Figure 40, two 22 μF X5R MLCC capacitors from Murata (GRM21BR60J226M) are sufficient for this application.

6. Because the ADP2106 is being used in this application, the input capacitors are 10 μF and 4.7 μF X5R Murata capacitors (GRM21BR61A106K and GRM21BR61A475K).
7. The input filter consists of a small 0.1 μF ceramic capacitor placed between IN and AGND and a 10 Ω resistor placed between IN and PWIN1.
8. Choose a soft start capacitor of 2 nF to achieve a soft start time of 2 ms.
9. Calculate the compensation resistor and capacitor as follows:

$$R_{COMP} = 0.8 \left(\frac{(2\pi)F_{CROSS}}{G_m G_{CS}} \right) \left(\frac{C_{OUT} V_{OUT}}{V_{REF}} \right) =$$

$$0.8 \left(\frac{(2\pi) \times 80 \text{ kHz}}{50 \mu\text{A/V} \times 2.8125 \text{ A/V}} \right) \left(\frac{30 \mu\text{F} \times 2 \text{ V}}{0.8 \text{ V}} \right) = 215 \text{ k}\Omega$$

$$C_{COMP} = \frac{2}{\pi F_{CROSS} R_{COMP}} = \frac{2}{\pi \times 80 \text{ kHz} \times 215 \text{ k}\Omega} = 39 \text{ pF}$$

EXTERNAL COMPONENT RECOMMENDATIONS

For popular output voltage options at 80 kHz crossover frequency with 10% overshoot for a 1 A load transient (refer to Figure 37 and Figure 38).

Table 11. Recommended External Components

Part	V _{OUT} (V)	C _{IN1} ¹ (μF)	C _{IN2} ¹ (μF)	C _{OUT} ² (μF)	L (μH)	R _{COMP} (kΩ)	C _{COMP} (pF)	R _{TOP} ³ (kΩ)	R _{BOT} ³ (kΩ)
ADP2105(ADJ)	0.9	4.7	4.7	22 + 10	2.0	135	82	5	40
ADP2105(ADJ)	1.2	4.7	4.7	22 + 4.7	2.5	135	82	20	40
ADP2105(ADJ)	1.5	4.7	4.7	10 + 10	3.0	135	82	35	40
ADP2105(ADJ)	1.8	4.7	4.7	10 + 10	3.3	135	82	50	40
ADP2105(ADJ)	2.5	4.7	4.7	10 + 4.7	3.6	135	82	85	40
ADP2105(ADJ)	3.3	4.7	4.7	10 + 4.7	4.1	135	82	125	40
ADP2106(ADJ)	0.9	4.7	10	22 + 10	1.5	90	100	5	40
ADP2106(ADJ)	1.2	4.7	10	22 + 4.7	1.8	90	100	20	40
ADP2106(ADJ)	1.5	4.7	10	10 + 10	2.0	90	100	35	40
ADP2106(ADJ)	1.8	4.7	10	10 + 10	2.2	90	100	50	40
ADP2106(ADJ)	2.5	4.7	10	10 + 4.7	2.5	90	100	85	40
ADP2106(ADJ)	3.3	4.7	10	10 + 4.7	3.0	90	100	125	40
ADP2107(ADJ)	0.9	10	10	22 + 10	1.2	70	120	5	40
ADP2107(ADJ)	1.2	10	10	22 + 4.7	1.5	70	120	20	40
ADP2107(ADJ)	1.5	10	10	10 + 10	1.5	70	120	35	40
ADP2107(ADJ)	1.8	10	10	10 + 10	1.8	70	120	50	40
ADP2107(ADJ)	2.5	10	10	10 + 4.7	1.8	70	120	85	40
ADP2107(ADJ)	3.3	10	10	10 + 4.7	2.5	70	120	125	40
ADP2105-1.2	1.2	4.7	4.7	22 + 4.7	2.5	135	82	N/A	N/A
ADP2105-1.5	1.5	4.7	4.7	10 + 10	3.0	135	82	N/A	N/A
ADP2105-1.8	1.8	4.7	4.7	10 + 10	3.3	135	82	N/A	N/A
ADP2105-3.3	3.3	4.7	4.7	10 + 4.7	4.1	135	82	N/A	N/A
ADP2106-1.2	1.2	4.7	10	22 + 4.7	1.8	90	100	N/A	N/A
ADP2106-1.5	1.5	4.7	10	10 + 10	2.0	90	100	N/A	N/A
ADP2106-1.8	1.8	4.7	10	10 + 10	2.2	90	100	N/A	N/A
ADP2106-3.3	3.3	4.7	10	10 + 4.7	3.0	90	100	N/A	N/A
ADP2107-1.2	1.2	10	10	22 + 4.7	1.5	70	120	N/A	N/A
ADP2107-1.5	1.5	10	10	10 + 10	1.5	70	120	N/A	N/A
ADP2107-1.8	1.8	10	10	10 + 10	1.8	70	120	N/A	N/A
ADP2107-3.3	3.3	10	10	10 + 4.7	2.5	70	120	N/A	N/A

¹ 4.7 μF 0805 X5R 10 V Murata—GRM21BR61A475KA73L. 10 μF 0805 X5R 10 V Murata—GRM21BR61A106KE19L.

² 4.7 μF 0805 X5R 10 V Murata—GRM21BR61A475KA73L. 10 μF 0805 X5R 10 V Murata—GRM21BR61A106KE19L. 22 μF 0805 X5R 6.3 V Murata—GRM21BR60J226ME39L.

³ 0.5% accuracy resistor.

For popular output voltage options at 80 kHz crossover frequency with 5% overshoot for a 1 A load transient (refer to Figure 37 and Figure 38).

Table 12. Recommended External Components

Part	V _{OUT} (V)	C _{IN1} ¹ (μF)	C _{IN2} ¹ (μF)	C _{OUT} ² (μF)	L (μH)	R _{COMP} (kΩ)	C _{COMP} (pF)	R _{TOP} ³ (kΩ)	R _{BOT} ³ (kΩ)
ADP2105(ADJ)	0.9	4.7	4.7	22 + 22 + 22	2.0	270	39	5	40
ADP2105(ADJ)	1.2	4.7	4.7	22 + 22 + 4.7	2.5	270	39	20	40
ADP2105(ADJ)	1.5	4.7	4.7	22 + 22	3.0	270	39	35	40
ADP2105(ADJ)	1.8	4.7	4.7	22 + 22	3.3	270	39	50	40
ADP2105(ADJ)	2.5	4.7	4.7	22 + 10	3.6	270	39	85	40
ADP2105(ADJ)	3.3	4.7	4.7	22 + 4.7	4.1	270	39	125	40
ADP2106(ADJ)	0.9	4.7	10	22 + 22 + 22	1.5	180	56	5	40
ADP2106(ADJ)	1.2	4.7	10	22 + 22 + 4.7	1.8	180	56	20	40
ADP2106(ADJ)	1.5	4.7	10	22 + 22	2.0	180	56	35	40
ADP2106(ADJ)	1.8	4.7	10	22 + 22	2.2	180	56	50	40
ADP2106(ADJ)	2.5	4.7	10	22 + 10	2.5	180	56	85	40
ADP2106(ADJ)	3.3	4.7	10	22 + 4.7	3.0	180	56	125	40
ADP2107(ADJ)	0.9	10	10	22 + 22 + 22	1.2	140	68	5	40
ADP2107(ADJ)	1.2	10	10	22 + 22 + 4.7	1.5	140	68	20	40
ADP2107(ADJ)	1.5	10	10	22 + 22	1.5	140	68	35	40
ADP2107(ADJ)	1.8	10	10	22 + 22	1.8	140	68	50	40
ADP2107(ADJ)	2.5	10	10	22 + 10	1.8	140	68	85	40
ADP2107(ADJ)	3.3	10	10	22 + 4.7	2.5	140	68	125	40
ADP2105-1.2	1.2	4.7	4.7	22 + 22 + 4.7	2.5	270	39	N/A	N/A
ADP2105-1.5	1.5	4.7	4.7	22 + 22	3.0	270	39	N/A	N/A
ADP2105-1.8	1.8	4.7	4.7	22 + 22	3.3	270	39	N/A	N/A
ADP2105-3.3	3.3	4.7	4.7	22 + 4.7	4.1	270	39	N/A	N/A
ADP2106-1.2	1.2	4.7	10	22 + 22 + 4.7	1.8	180	56	N/A	N/A
ADP2106-1.5	1.5	4.7	10	22 + 22	2.0	180	56	N/A	N/A
ADP2106-1.8	1.8	4.7	10	22 + 22	2.2	180	56	N/A	N/A
ADP2106-3.3	3.3	4.7	10	22 + 4.7	3.0	180	56	N/A	N/A
ADP2107-1.2	1.2	10	10	22 + 22 + 4.7	1.5	140	68	N/A	N/A
ADP2107-1.5	1.5	10	10	22 + 22	1.5	140	68	N/A	N/A
ADP2107-1.8	1.8	10	10	22 + 22	1.8	140	68	N/A	N/A
ADP2107-3.3	3.3	10	10	22 + 4.7	2.5	140	68	N/A	N/A

¹ 4.7μF 0805 X5R 10V Murata—GRM21BR61A475KA73L. 10μF 0805 X5R 10V Murata—GRM21BR61A106KE19L.

² 4.7μF 0805 X5R 10V Murata—GRM21BR61A475KA73L. 10μF 0805 X5R 10V Murata—GRM21BR61A106KE19L. 22μF 0805 X5R 6.3V Murata—GRM21BR60J226ME39L.

³ 0.5% accuracy resistor.

CIRCUIT BOARD LAYOUT RECOMMENDATIONS

Good circuit board layout is essential to obtaining the best performance from the ADP2105/ADP2106/ADP2107. Poor circuit layout degrades the output ripple, as well as the electromagnetic interference (EMI) and electromagnetic compatibility (EMC) performance.

Figure 54 and Figure 55 show the ideal circuit board layout for the ADP2105/ADP2106/ADP2107 to achieve the highest performance. Refer to the following guidelines if adjustments to the suggested layout are needed:

- Use separate analog and power ground planes. Connect the ground reference of sensitive analog circuitry (such as compensation and output voltage divider components) to analog ground; connect the ground reference of power components (such as input and output capacitors) to power ground. In addition, connect both the ground planes to the exposed pad of the ADP2105/ADP2106/ADP2107.
- For each PWIN pin, place an input capacitor as close to the PWIN pin as possible and connect the other end to the closest power ground plane.
- Place the 0.1 μF , 10 Ω low-pass input filter between the IN pin and the PWIN1 pin, as close to the IN pin as possible.
- Ensure that the high current loops are as short and as wide as possible. Make the high current path from C_{IN} through L, C_{OUT} , and the PGND plane back to C_{IN} as short as possible. To accomplish this, ensure that the input and output capacitors share a common PGND plane.
- Make the high current path from the PGND pin through L and C_{OUT} back to the PGND plane as short as possible. To accomplish this, ensure that the PGND pin is tied to the PGND plane as close as possible to the input and output capacitors.
- The feedback resistor divider network is to be placed as close as possible to the FB pin to prevent noise pickup. The length of trace connecting the top of the feedback resistor divider to the output is to be as short as possible while keeping away from the high current traces and the LX (switch) node that can lead to noise pickup. An analog ground plane is to be placed on either side of the FB trace to reduce noise pickup. For the low fixed voltage options (1.2 V and 1.5 V), poor routing of the OUT_SENSE trace can lead to noise pickup, adversely affecting load regulation. This can be fixed by placing a 1 nF bypass capacitor close to the FB pin.
- The placement and routing of the compensation components are critical for proper behavior of the ADP2105/ADP2106/ADP2107. The compensation components are to be placed as close to the COMP pin as possible. It is advisable to use 0402-sized compensation components for closer placement, leading to smaller parasitics. Surround the compensation components with an analog ground plane to prevent noise pickup. The metal layer under the compensation components is to be the analog ground plane.

EVALUATION BOARD

EVALUATION BOARD SCHEMATIC FOR ADP2107 (1.8 V)

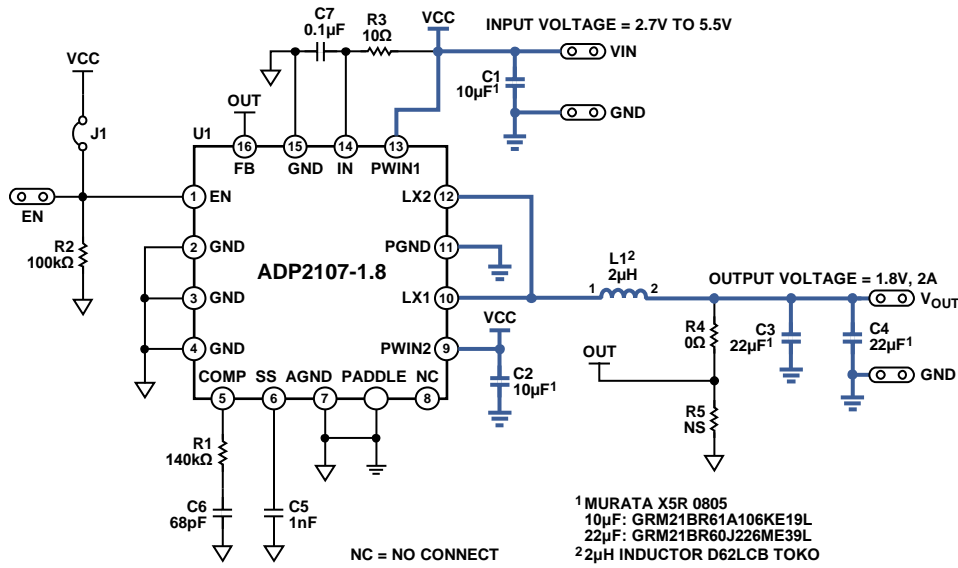


Figure 53. Evaluation Board Schematic of the ADP2107-1.8 (Bold Traces are High Current Paths)

RECOMMENDED PCB LAYOUT (EVALUATION BOARD LAYOUT)

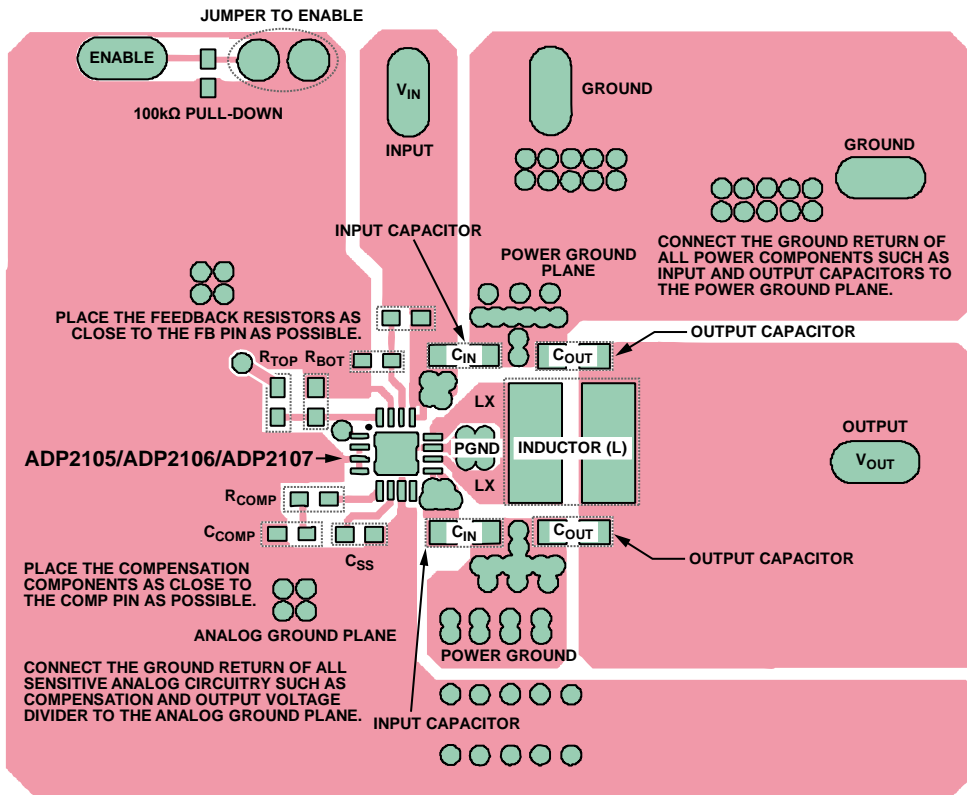
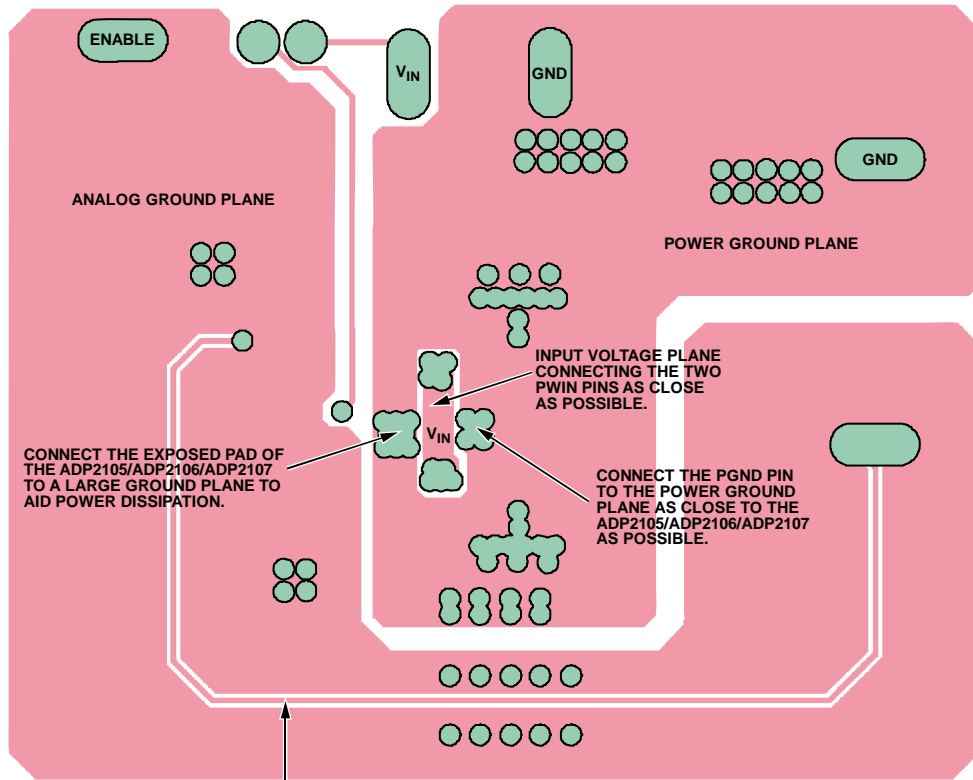


Figure 54. Recommended Layout of Top Layer of ADP2105/ADP2106/ADP2107



CONNECT THE EXPOSED PAD OF THE ADP2105/ADP2106/ADP2107 TO A LARGE GROUND PLANE TO AID POWER DISSIPATION.

INPUT VOLTAGE PLANE CONNECTING THE TWO PWIN PINS AS CLOSE AS POSSIBLE.

CONNECT THE PGND PIN TO THE POWER GROUND PLANE AS CLOSE TO THE ADP2105/ADP2106/ADP2107 AS POSSIBLE.

FEEDBACK TRACE: THIS TRACE CONNECTS THE TOP OF THE RESISTIVE VOLTAGE DIVIDER ON THE FB PIN TO THE OUTPUT. PLACE THIS TRACE AS FAR AWAY FROM THE LX NODE AND HIGH CURRENT TRACES AS POSSIBLE TO PREVENT NOISE PICKUP.

Figure 55. Recommended Layout of Bottom Layer of ADP2105/ADP2106/ADP2107

98079-046

APPLICATION CIRCUITS

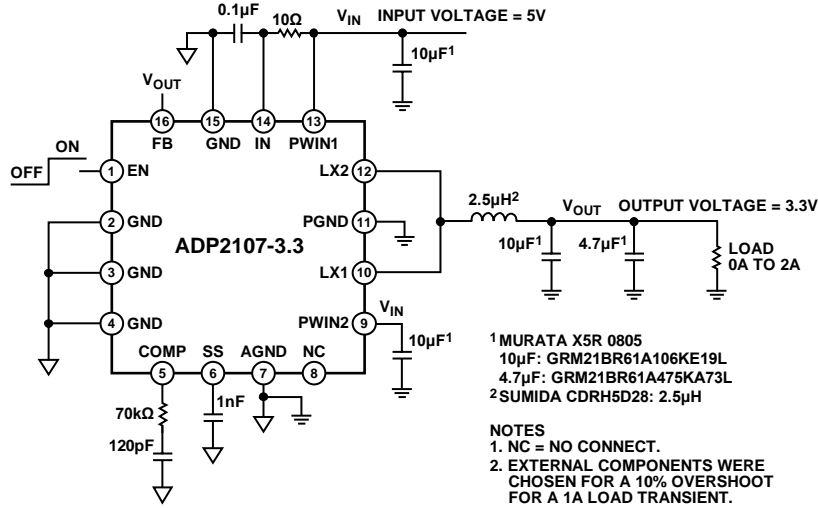


Figure 56. Application Circuit— $V_{IN} = 5V$, $V_{OUT} = 3.3V$, Load = 0 A to 2 A

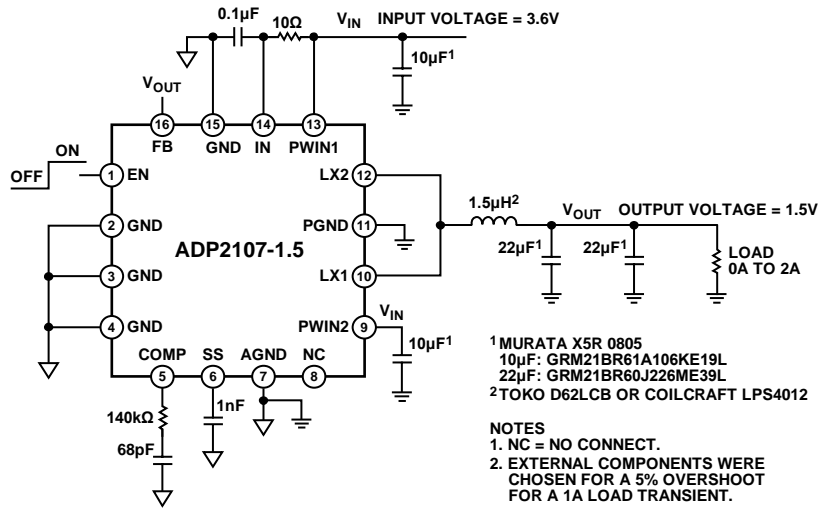


Figure 57. Application Circuit— $V_{IN} = 3.6V$, $V_{OUT} = 1.5V$, Load = 0 A to 2 A

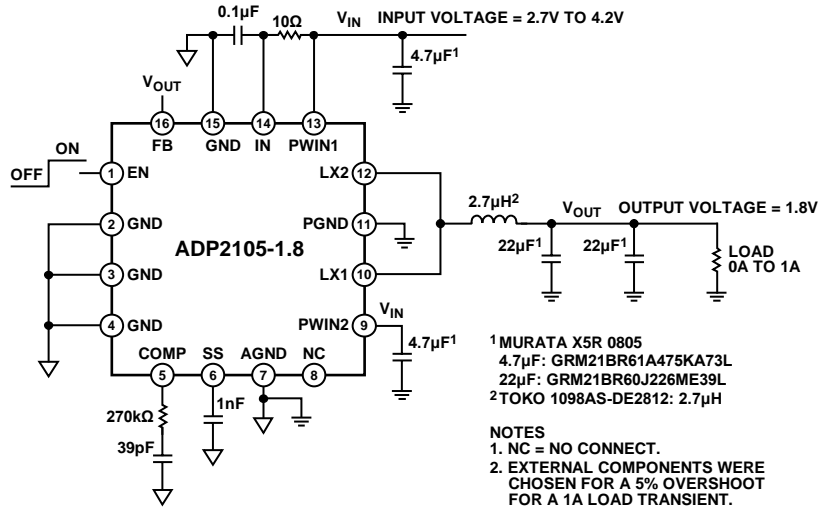


Figure 58. Application Circuit— V_{IN} = Li-Ion Battery, V_{OUT} = 1.8 V, Load = 0 A to 1 A

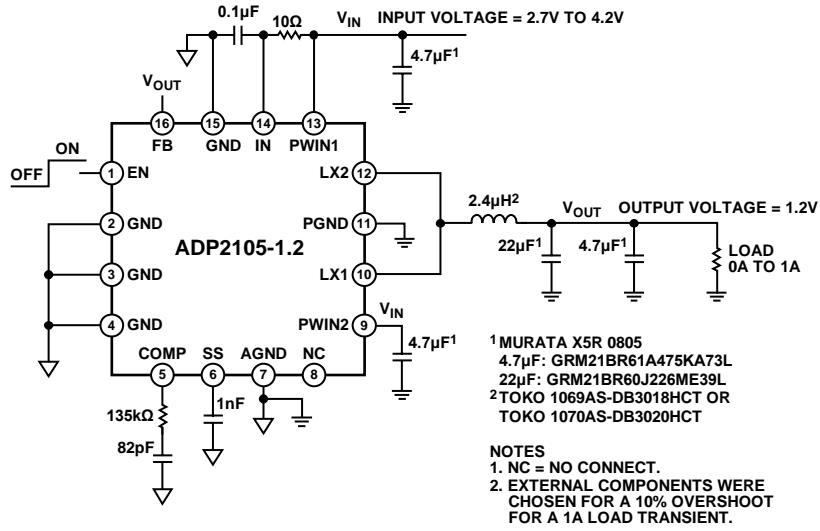


Figure 59. Application Circuit— V_{IN} = Li-Ion Battery, V_{OUT} = 1.2 V, Load = 0 A to 1 A

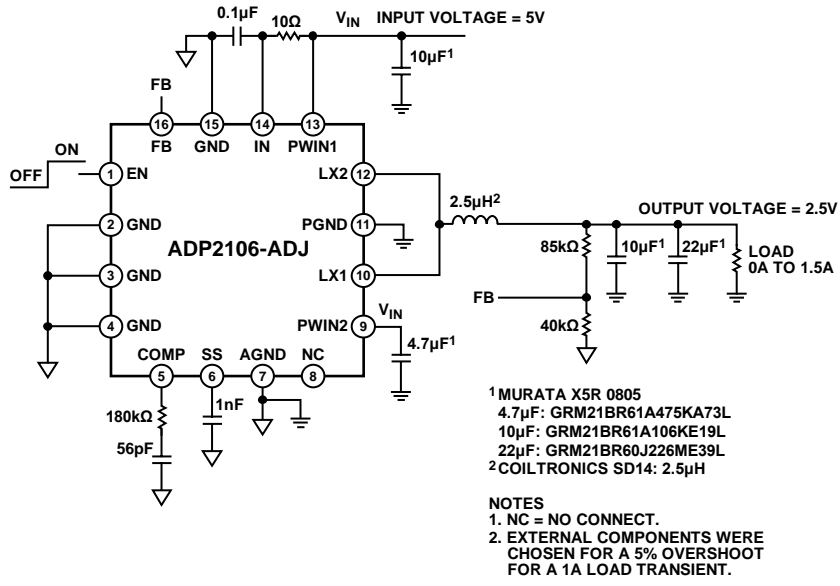
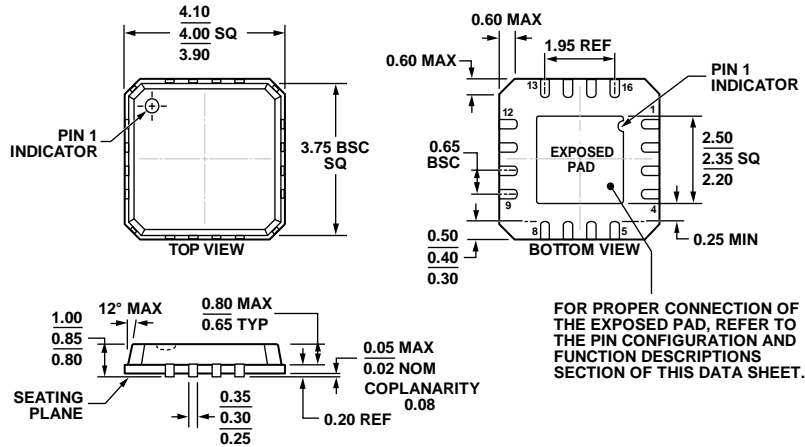


Figure 60. Application Circuit— $V_{IN} = 5V$, $V_{OUT} = 2.5V$, Load = 0A to 1.5A

08079-401

OUTLINE DIMENSIONS



COMPLIANT TO JEDEC STANDARDS MO-220-VGGC

Figure 61. 16-Lead Lead Frame Chip Scale Package [LFCSQ_VQ]
 4 mm × 4 mm Body, Very Thin Quad
 (CP-16-10)
 Dimensions shown in millimeters

04-06-2012-A

ORDERING GUIDE

Model ¹	Output Current	Temperature Range	Output Voltage	Package Description	Package Option
ADP2105ACPZ-1.2-R7	1 A	-40°C to +125°C	1.2 V	16-Lead LFCSP_VQ	CP-16-10
ADP2105ACPZ-1.5-R7	1 A	-40°C to +125°C	1.5 V	16-Lead LFCSP_VQ	CP-16-10
ADP2105ACPZ-1.8-R7	1 A	-40°C to +125°C	1.8 V	16-Lead LFCSP_VQ	CP-16-10
ADP2105ACPZ-3.3-R7	1 A	-40°C to +125°C	3.3 V	16-Lead LFCSP_VQ	CP-16-10
ADP2105ACPZ-R7	1 A	-40°C to +125°C	ADJ	16-Lead LFCSP_VQ	CP-16-10
ADP2106ACPZ-1.2-R7	1.5 A	-40°C to +125°C	1.2 V	16-Lead LFCSP_VQ	CP-16-10
ADP2106ACPZ-1.5-R7	1.5 A	-40°C to +125°C	1.5 V	16-Lead LFCSP_VQ	CP-16-10
ADP2106ACPZ-1.8-R7	1.5 A	-40°C to +125°C	1.8 V	16-Lead LFCSP_VQ	CP-16-10
ADP2106ACPZ-3.3-R7	1.5 A	-40°C to +125°C	3.3 V	16-Lead LFCSP_VQ	CP-16-10
ADP2106ACPZ-R7	1.5 A	-40°C to +125°C	ADJ	16-Lead LFCSP_VQ	CP-16-10
ADP2107ACPZ-1.2-R7	2 A	-40°C to +125°C	1.2 V	16-Lead LFCSP_VQ	CP-16-10
ADP2107ACPZ-1.5-R7	2 A	-40°C to +125°C	1.5 V	16-Lead LFCSP_VQ	CP-16-10
ADP2107ACPZ-1.8-R7	2 A	-40°C to +125°C	1.8 V	16-Lead LFCSP_VQ	CP-16-10
ADP2107ACPZ-3.3-R7	2 A	-40°C to +125°C	3.3 V	16-Lead LFCSP_VQ	CP-16-10
ADP2107ACPZ-R7	2 A	-40°C to +125°C	ADJ	16-Lead LFCSP_VQ	CP-16-10
ADP2105-1.8-EVALZ			1.8 V	Evaluation Board	
ADP2105-EVALZ			Adjustable, but set to 2.5 V	Evaluation Board	
ADP2106-1.8-EVALZ			1.8 V	Evaluation Board	
ADP2106-EVALZ			Adjustable, but set to 2.5 V	Evaluation Board	
ADP2107-1.8-EVALZ			1.8 V	Evaluation Board	
ADP2107-EVALZ			Adjustable, but set to 2.5 V	Evaluation Board	

¹Z = RoHS Compliant Part.

NOTES

NOTES

NOTES

Компания «Океан Электроники» предлагает заключение долгосрочных отношений при поставках импортных электронных компонентов на взаимовыгодных условиях!

Наши преимущества:

- Поставка оригинальных импортных электронных компонентов напрямую с производств Америки, Европы и Азии, а так же с крупнейших складов мира;
- Широкая линейка поставок активных и пассивных импортных электронных компонентов (более 30 млн. наименований);
- Поставка сложных, дефицитных, либо снятых с производства позиций;
- Оперативные сроки поставки под заказ (от 5 рабочих дней);
- Экспресс доставка в любую точку России;
- Помощь Конструкторского Отдела и консультации квалифицированных инженеров;
- Техническая поддержка проекта, помощь в подборе аналогов, поставка прототипов;
- Поставка электронных компонентов под контролем ВП;
- Система менеджмента качества сертифицирована по Международному стандарту ISO 9001;
- При необходимости вся продукция военного и аэрокосмического назначения проходит испытания и сертификацию в лаборатории (по согласованию с заказчиком);
- Поставка специализированных компонентов военного и аэрокосмического уровня качества (Xilinx, Altera, Analog Devices, Intersil, Interpoint, Microsemi, Actel, Aeroflex, Peregrine, VPT, Syfer, Eurofarad, Texas Instruments, MS Kennedy, Miteq, Cobham, E2V, MA-COM, Hittite, Mini-Circuits, General Dynamics и др.);

Компания «Океан Электроники» является официальным дистрибьютором и эксклюзивным представителем в России одного из крупнейших производителей разъемов военного и аэрокосмического назначения «**JONHON**», а так же официальным дистрибьютором и эксклюзивным представителем в России производителя высокотехнологичных и надежных решений для передачи СВЧ сигналов «**FORSTAR**».



JONHON

«**JONHON**» (основан в 1970 г.)

Разъемы специального, военного и аэрокосмического назначения:

(Применяются в военной, авиационной, аэрокосмической, морской, железнодорожной, горно- и нефтедобывающей отраслях промышленности)

«**FORSTAR**» (основан в 1998 г.)

ВЧ соединители, коаксиальные кабели,
кабельные сборки и микроволновые компоненты:

(Применяются в телекоммуникациях гражданского и специального назначения, в средствах связи, РЛС, а так же военной, авиационной и аэрокосмической отраслях промышленности).



Телефон: 8 (812) 309-75-97 (многоканальный)

Факс: 8 (812) 320-03-32

Электронная почта: ocean@oceanchips.ru

Web: <http://oceanchips.ru/>

Адрес: 198099, г. Санкт-Петербург, ул. Калинина, д. 2, корп. 4, лит. А